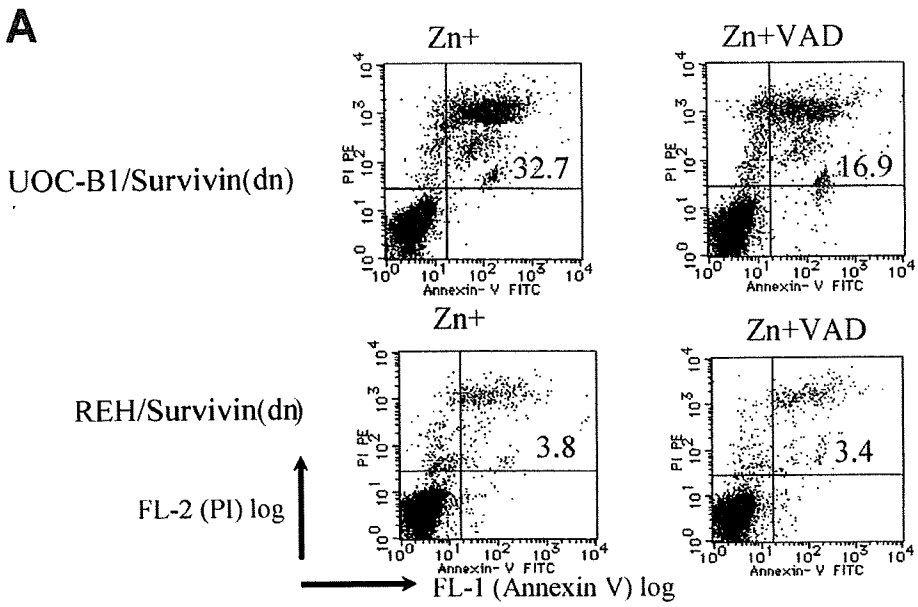

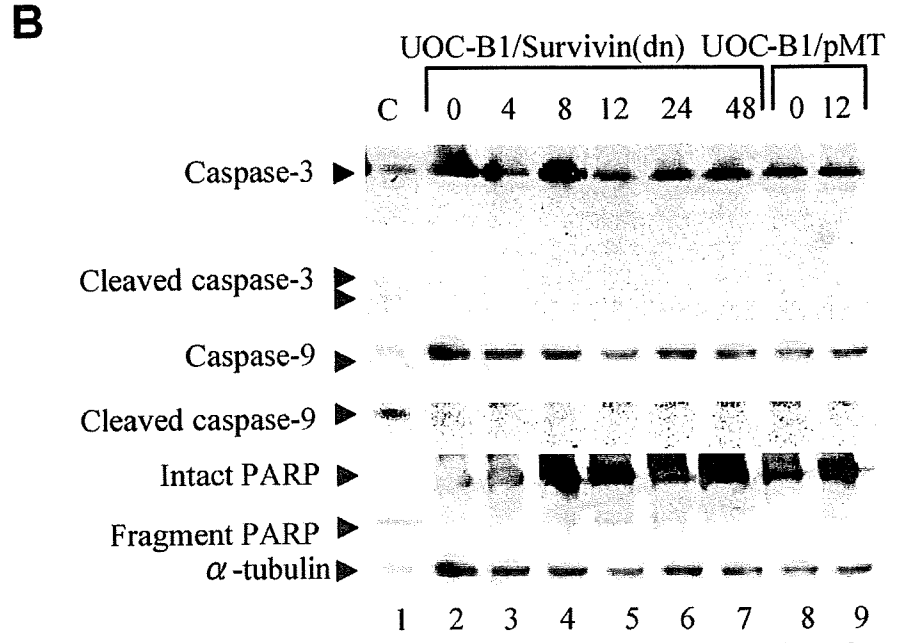

FIGURE 5. **PARP activation in Survivin(dn)-expressing cells and effect of caspase inhibitor.** *A*, flow cytometric analysis stained with annexin-V (*abscissa*) and PI (*ordinate*). UOC-B1/Survivin(dn) and REH/Survivin(dn) cells were cultured in medium containing 100 μM zinc 1 h after treatment with or without 20 μM benzyloxycarbonyl-VAD-fluoromethyl ketone (*VAD*), a pan-caspase inhibitor. *B*, UOC-B1/Survivin(dn) or UOC-B1/pMT cells were cultured in medium containing 100 μM zinc for the indicated times. Immunoblot analysis of UOC-B1/Survivin(dn) cells was performed to detect caspase-3, cleaved caspase-3, caspase-9, cleaved caspase-9, intact PARP, fragmented PARP, and α-tubulin proteins. As a positive control (C), Jurkat cells were treated with etoposide.

ceded the reduction of Survivin mRNA (Fig. 1*D*), suggesting the involvement of post-transcriptional mechanism(s).

Cell Cycle-independent Induction of Survivin by E2A-HLF—The Survivin mRNA and protein levels at the G_2/M phase of the cell cycle are more than 10-fold higher than those at the G_1 phase in NIH3T3 murine fibroblasts synchronized by serum starvation and in drug-synchronized HeLa cells (17, 25). Because it is difficult to synchronize leukemia cells by serum starvation or by reagents inhibiting cell cycle progression at a specific phase, we performed counterflow centrifugal elutriation to enrich cells at each phase of the cell cycle. The purity of the preparations was typically more than 90% for G_0/G_1-phase cells, more than 80% for S-phase cells, and ~90% for G_2/M-phase cells (Fig. 2*A*). We performed immunoblot analysis to measure Survivin expression in the enriched fractions. In t(17;19)$^-$ ALL cell lines (RS4;11, REH, and 920), Survivin expression was most evident at the G_2/M-phase (Fig. 2, *B*, *lanes 13–21*, and *C*). In particular, 920 cells at the G_2/M phase showed ~11- and 4-fold higher expression than those at the G_1 and S phase, respectively. By contrast, the four cell lines harboring the E2A-HLF chimeric protein expressed Survivin at high levels throughout the cell cycle (Fig. 2, *B*, *lanes 1–12*, and *C*).

E2A-HLF Enhances the Promoter Activity of the Survivin Gene—To elucidate how E2A-HLF induces expression of the *survivin* gene, we analyzed the effects of E2A-HLF on the function of the *survivin* promoter. We initially generated reporter plasmid vectors (pGL3-124, -190, -265, -480, and -675), each of which contained a different length of human *survivin* promoter. These vectors were analyzed for luciferase activity in transiently transfected Nalm-6/E2A-HLF cells. When cells were cultured without zinc, luciferase activity was low in cells transfected with pGL3-124 (Fig. 3*A*). Transfection of pGL3-190 resulted in the highest luciferase activity; it was nearly 6-fold higher than that which resulted from transfection of pGL3-124. However, transfection of *survivin* constructs longer than pGL3-265 resulted in significantly less activity compared with that of pGL3-190, suggesting the presence of enhancer elements in the region from nt −124 to −190 and repressor elements in the region upstream of nt −190. When cells were cultured with zinc for 24 h, the luciferase activity of each reporter construct, including the shortest pGL3-124, increased by ~3-fold compared with the respective cells cultured without zinc, suggesting that E2A-HLF induces *survivin* transcription through *cis* elements in the region from nt 0 to −124.

To further investigate the mechanism through which E2A-HLF induces transcription of the *survivin* gene, we used luciferase reporter constructs with mutated cell cycle-dependent *cis* elements. These elements, including the cell cycle-dependent element (CDE; GGCGG) and the cell cycle homology region (CHR; ATTTGAA), are implicated in G_1 transcriptional repression in S/G_2-regulated genes, such as cyclin A, cdc25C, and cdc2 (18). A previously published report demonstrated two CDEs (−6 and −12) and one CHR (−42) in the human *survivin* promoter between nt 0 and −124 (Fig. 3*B*) (18). When pGL3-124mut1, which contained mutated CDE-6 and CDE-12 but had intact CHR-42, was transfected in Nalm-6/E2A-HLF cells, the level of luciferase activity was virtually the same as that of pGL3-124 regardless of the presence of zinc, suggesting that CDE-6 and CDE-12 do not contribute to regulation of *survivin* transcription in Nalm-6 cells (Fig. 3*A*). By contrast, transfection of pGL3-124mut2, which contained mutated CHR-42 in addition to mutated CDE-6 and CDE-12, resulted in 10-fold higher luciferase activity in the absence of zinc and 3-fold higher luciferase activity in the presence of zinc compared with transfection of pGL3-124. As a result, there was virtually no difference in the level of luciferase activity between the presence or absence of zinc in cells transfected with pGL3-124mut2. Transfection of pGL3-124mut3, in which only CHR-42 was mutated, show similar results as transfection of pGL3-124mut2. These results suggested that E2A-HLF directly or indirectly up-regulates transcription of *survivin* through a CHR-42 silencer.

To elucidate transcription factors that bind to CHR-42, we performed EMSA. Smear-looking CHR probe-protein complexes were readily detected (Fig. 3*C*, *lane 1*) and were ablated by the addition of an excess amount of cold competitor (*lane 3*) but not by mutated CHR competitor (*lane 4*). These complexes were not detected when using mutated CHR as a probe (Fig. 3*C*, *lane 5*), suggesting that this complex represents specific binding between transcription factor(s) and the CHR sequence. When E2A-HLF was induced by the addition of zinc, the intensity of the smear decreased (Fig. 3*C*, *lane 2*), further supporting that E2A-HLF up-regulates expression of *survivin* via a CHR-42 silencer.

Specific Inhibition of Survivin-induced Apoptosis in t(17;19)$^+$ ALL Cell Lines—To test whether induction of Survivin by E2A-HLF is essential for the survival of t(17;19)$^+$ leukemia cells, we initially used zinc-inducible expression of a phosphorylation-defective Survivin mutant (Survivin-T34A) that functions as a dominant negative inhibitor. An annexin-V binding assay was used to measure externalization of phosphatidylserine, an indicator of cell death. Ectopic expression of Survivin-T34A in two t(17;19)$^+$ ALL cell lines (UOC-B1 and Endo-kun) caused a rapid increase in the fraction of annexin-V-positive cells within 24 h after the addition of zinc (Fig. 4*A*). In control UOC-B1/pMT and Endo-kun/pMT cells, which contained the empty vector, less than 20% of cells were positive for annexin-V regardless of the presence of zinc. By contrast, Survivin-T34A did not induce massive cell death in two t(17;19)$^-$ leukemia cell lines (REH and Jurkat), which express relatively high levels of Survivin (Fig. 1*A*). The basis for the altered survival of UOC-B1 and Endo-kun cells expressing Survivin-T34A was investigated by TUNEL analysis using flow cytometry. BrdUrd uptake (Fig. 4*B*, *x* axis) by TdT that reflects a number of DNA ends in each cell was markedly increased in UOC-B1 and Endo-kun cells expressing Survivin-T34A. Interestingly, intensities of BrdUrd signals increased equally in cells at each cell cycle phase (*y* axis), suggesting that down-regulation of Survivin function induces apoptosis in a cell cycle-independent manner. By contrast, expression of Survivin-T34A did not induce apoptosis in REH cells and induced apoptosis in Jurkat cells only at the G_2/M phase (Fig. 4*B*).

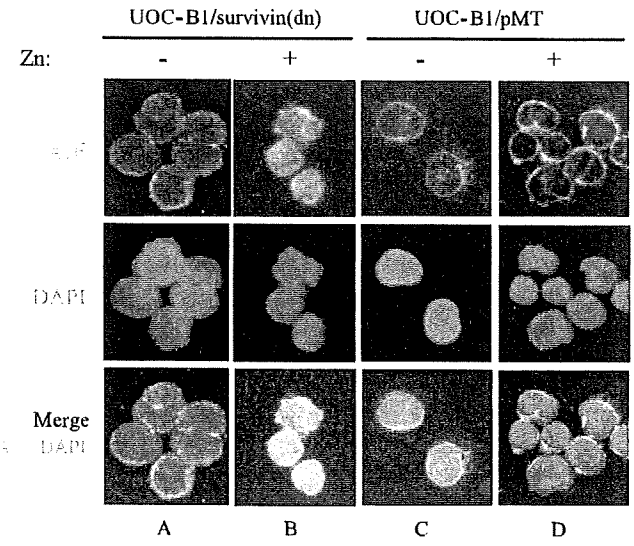

FIGURE 6. **Effect of Survivin(dn) on nuclear translocation of AIF.** UOC-B1/Survivin(dn) cells (*A* and *B*) or UOC-B1/pMT cells (*C* and *D*) were cultured for 12 h in the absence of zinc (*A* and *C*) or in the presence of 100 μM zinc (*B* and *D*). Cells were immunostained with an anti-AIF polyclonal antibody (*upper panels*). Cells were stained with 4′,6-diamidino-2-phenylindole (*DAPI*) to visualize the nuclei (*middle* and *lower panels*).

We next down-regulated Survivin by lentivirally introduced short hairpin (sh) RNA. The Survivin protein expression level in cells sorted by expression of GFP (as an indicator of infection) was significantly reduced by Survivin-shRNA1 and -3–5 compared with that in cells infected with control-shRNA (Fig. 4*C*). We introduced shRNA1 or -5 into REH, UOC-B1, and Endo-kun cells. Twenty four hours later, when about 10% of the cells were GFP-positive, dead cells were determined by annexin-V and 7-AAD staining. Marked increases in annexin-V- and 7-AAD-positive cells were detected in the GFP-positive population of UOC-B1 or Endo-kun cells compared with those in GFP-positive REH cells (Fig. 4*D*).

Caspase-dependent and -independent Cell Death Are Induced by Survivin-T34A in t(17;19)$^+$ Cells—To elucidate the molecular mechanisms through which Survivin protects t(17;19)$^+$ ALL cells from apoptosis, we initially examined caspase-dependent pathways. A pan-caspase inhibitor, benzyloxycarbonyl-VAD-fluoromethyl ketone, partially blocked cell death induced by Survivin-T34A (Fig. 5*A*). Immunoblot analysis revealed fragmentation of PARP within 8 h after induction of Survivin-T34A, although cleavage of caspase-3 and -9 was barely detectable up through 48 h (Fig. 5*B*). These results suggested that caspase-independent pathways contribute to cell death induced by Survivin-T34A in t(17;19)$^+$ ALL cells.

The association of Survivin targeting both preceding and independent of caspase activation suggested to us a potential role for AIF, given its capacity to mediate DNA fragmentation

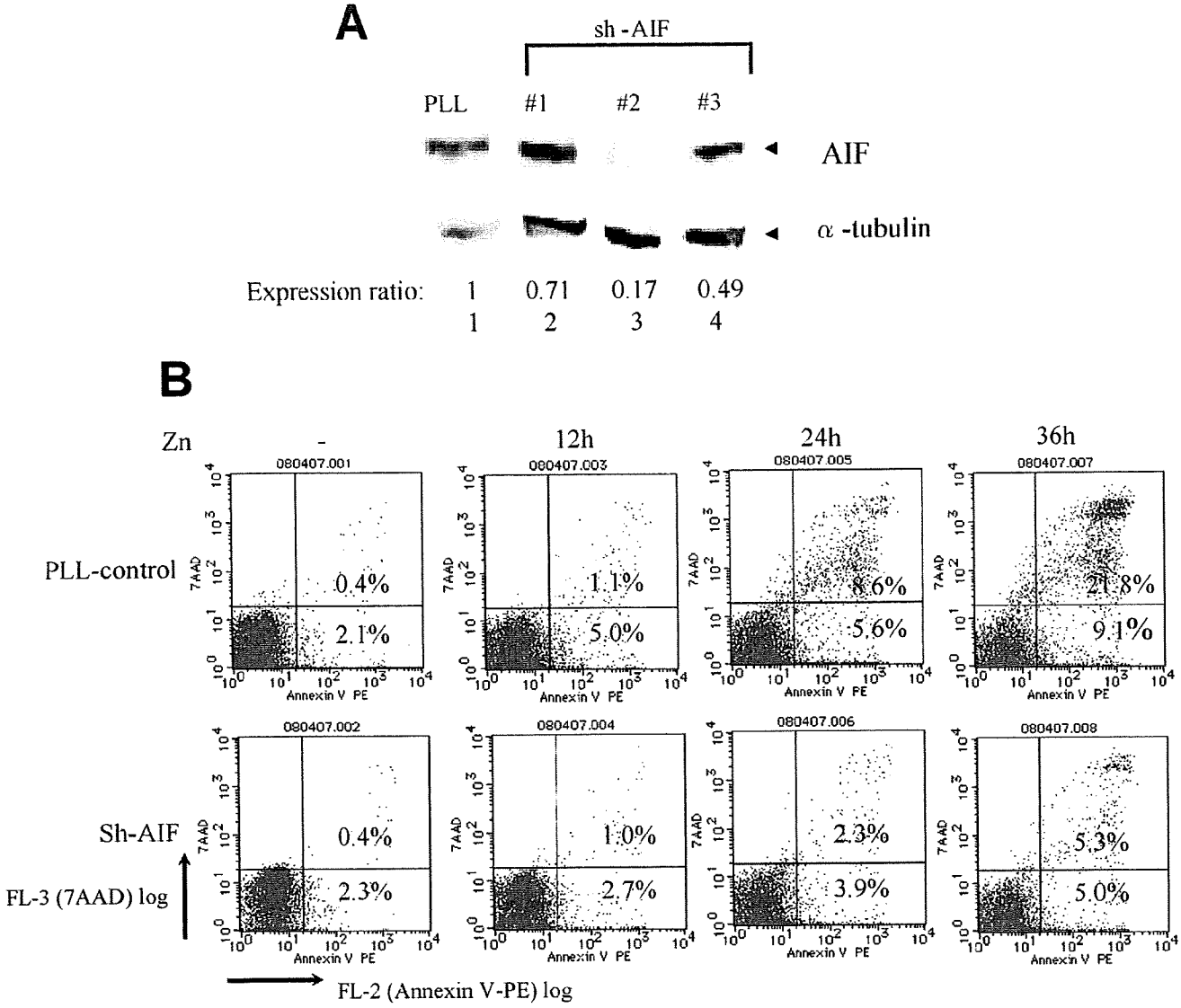

FIGURE 7. **Inhibition of Survivin-T34A-induced apoptosis by knockdown of AIF.** *A*, immunoblot analysis using AIF (*upper panel*) or α-tubulin (*lower panel*) antibodies. UOC-B1/Survivin(dn) cells were infected with lentivirus expressing the shRNA indicated *above* each panel, and GFP-positive cells were sorted. Ratios of intensity are shown *below*. *B*, UOC-B1/Survivin(dn) cells were infected with lentivirus expressing control-shRNA (*PLL*, *upper*) or AIF-shRNA2 (*lower*), cultured with 100 μM zinc for the indicated length of time, and stained with annexin-V-phycoerythrin (*PE*) (*abscissa*) and 7-AAD (*ordinate*). The data show the ratio of annexin-V-phycoerythrin- and 7-AAD-positive cells in the GFP-positive fraction as determined by flow cytometric analysis. *Numbers* indicate the percentage of apoptotic cells.

and cytochrome *c* release in a caspase-independent fashion (28, 29). We analyzed the nuclear translocation of AIF after induction of Survivin-T34A in t(17;19)$^+$ ALL cells. In the UOC-B1/Survivin(dn) cells without induction of Survivin-T34A, AIF signals were found in the cytoplasm in ~75% of the total cell population (Fig. 6*A*), consistent with a previous report showing the presence of AIF in mitochondria (27). By contrast, expression of Survivin-T34A for 12 h induced nuclear translocation of AIF signals in more than 90% of cells (Fig. 6*B*). Nuclear translocation of AIF was induced in only a small percentage (~ 4%) of the control UOC-B1/pMT cells treated with zinc (Fig. 6*D*).

To test the role of AIF in cell death induced by Survivin-T34A in t(17;19)$^+$ ALL cells, we down-regulated AIF expression by lentivirally expressed AIF-shRNA. The AIF protein expression level in UOC-B1/Survivin(dn) cells was significantly reduced by AIF-shRNA2 compared with that in cells infected with control PLL-shRNA sorted by expression of GFP (Fig. 7*A*). The number of cells undergoing cell death by induction of Survivin-T34A was monitored by annexin-V and 7-AAD staining in GFP-positive cells. Cells treated with AIF-shRNA2 were significantly resistant to cell death compared with those treated with control PLL-shRNA (Fig. 7*B*), suggesting that AIF plays critical roles in Survivin-mediated cell death of t(17;19)$^+$ ALL cells.

DISCUSSION

We previously demonstrated that E2A-HLF contributes to leukemogenesis of t(17;19)-positive ALL through inhibition of apoptosis (6). Here, we demonstrate that E2A-HLF induces Survivin expression through transcriptional regulation. Down-

regulation of Survivin function by a dominant negative mutant of Survivin (Survivin-T34A) or reduction of Survivin expression by shRNA induced massive apoptosis in t(17;19)$^+$ leukemia cells throughout the cell cycle. Down-regulation of Survivin induced apoptosis via both caspase-dependent and -independent pathways, and AIF was involved in the latter pathways. These findings indicate that Survivin plays critical roles in E2A-HLF-mediated leukemogenesis.

E2A-HLF, known as a *trans*-activator (24), could either directly or indirectly enhance *survivin* transcription. However, there is no potential binding site of E2A-HLF (GTTACGTAAT) in the promoter region of *survivin*, and indeed, no binding activity of E2A-HLF was detected by EMSA in the immediate upstream region (124 bp) of the initial ATG, including a region that contains CHR-42 sequence (ATTTGAA) (negative data not shown). Thus, E2A-HLF most likely inhibits the silencer activity of CHR-42 (Fig. 3*A*) by down-regulating a certain amount of hypothetical *trans*-repressor *X* that binds to CHR-42 (Fig. 3*C*, *lane 2*). Theoretically, E2A-HLF may induce another *trans*-repressor that down-regulates the expression of *trans*-repressor *X*. Alternatively, a downstream target factor of E2A-HLF may reduce the DNA binding potential of *trans*-repressor *X*. It is of interest to note that whether or not the mechanism through which E2A-HLF induces *survivin* transcription is common to that, Ras pathways regulate Survivin expression. As we reported previously (30), because downstream targets of Ras enhance Survivin expression through enhancer(s) between −124 to −190, E2A-HLF likely induces Survivin through distinctive pathways.

Previous reports indicated that Survivin inhibits apoptosis through both caspase-dependent and caspase-independent pathways, although detailed mechanisms are not yet understood (31–34). In t(17;19)$^+$ ALL cells undergoing apoptosis by Survivin-T34A, activation of the caspase cascade is likely a secondary event, because activated caspase-3 and -9 were not detectable up through 48 h after induction of Survivin-T34A (Fig. 5*B*), even though the cells were positive on annexin-V staining and TUNEL analysis within 12 h (Fig. 4, *A* and *B*). We observed rapid PARP activation within 8 h that is required for translocation of AIF to the nucleus from mitochondria, followed by morphological changes such as cell shrinkage and chromatin condensation (27, 35). Moreover, knockdown of AIF in UOC-B1/Survivin(dn) cells protected cells from apoptosis induced by Survivin-T34A (Fig. 7*B*). Therefore, reversal of AIF translocation by Survivin, which is induced by E2A-HLF throughout the cell cycle, appears to be the key mechanism in the protection of t(17;19)$^+$ leukemia cells from apoptosis.

In earlier studies, we identified *SLUG* as a target gene of E2A-HLF (36). SLUG is a transcription factor closely related to Ces-1, a cell death regulator in *Caenorhabditis elegans* (36, 37). Importantly, *ces-1* is a downstream target gene of *ces-2*, which is closely related to E2A-HLF (6, 38). The apparent convergence of cell death pathways, including CES-2/CES-1 in the worm and E2A-HLF/SLUG in human pro-B leukemia (6, 36), suggests that SLUG may have an important regulatory role in the survival of lymphoid cells. However, the lack of expression of Slug by normal pro-B cells suggests that E2A-HLF acts not by invoking a normal survival pathway in B lymphocytes but rather by aberrantly activating a Slug-mediated survival pathway normally used by more primitive hematopoietic cell progenitors (39). Therefore, it is still uncertain whether only the E2A-HLF/SLUG pathway inhibits apoptosis in leukemia pro-B cell progenitors (36). Perhaps E2A-HLF has multiple apoptosis-inhibiting pathways to coordinate leukemogenesis.

t(17;19)$^+$ ALL almost always proves refractory to intensive chemotherapy, even to the aggressive conditioning for bone marrow transplantation (3–5). Survivin is an attractive therapeutic target in t(17;19)$^+$ ALLs because of its differential expression in tumors *versus* normal tissues and because it may be required for maintaining cell viability in this leukemia (14, 16). The efficacy of Survivin antisense oligonucleotides has been demonstrated *in vivo* (40, 41), and clinical grade antisense Survivin oligonucleotides are currently under development (42, 43). Although Survivin is not a cancer-specific molecule in regulating normal cell function particularly in the hematopoietic stem cell and immune systems, anti-Survivin therapies developed to date have not revealed major systemic toxicities in animal models and are encouraging (44). Our results provide further evidence that Survivin inhibitors may be an effective therapeutic strategy for this refractory ALL.

Acknowledgments—We thank M. Eguchi for helpful discussions, support, and encouragement throughout this study and Y. Sato for support and encouragement. We thank F. J. Rauscher III for providing the pMT-CB6$^+$ expression vector; K. Harada, H. Aoyama, and M. Ishiguchi for excellent technical assistance; K. Ohyashiki and K. Toyama for HAL-01 cell lines; and M. Endo for Endo-kun cell lines.

REFERENCES

1. Inaba, T., Roberts, W. M., Shapiro, L. H., Jolly, K. W., Raimondi, S. C., Smith, S. D., and Look, A. T. (1992) *Science* **257,** 531–534
2. Hunger, S. P., Ohyashiki, K., Toyama, K., and Cleary, M. L. (1992) *Genes Dev.* **6,** 1608–1620
3. Hunger, S. P. (1996) *Blood* **87,** 1211–1224
4. Inukai, T., Hirose, K., Inaba, T., Kurosawa, H., Hama, A., Inada, H., Chin, M., Nagatoshi, Y., Ohtsuka, Y., Oda, M., Goto, H., Endo, M., Morimoto, A., Imaizumi, M., Kawamura, N., Miyajima, Y., Ohtake, M., Miyaji, R., Saito, M., Tawas, A., Yanai, F., Goi, K., Nakazawa, S., and Sugita, K. (2007) *Leukemia* **21,** 288–296
5. Matsunaga, T., Inaba, T., Matsui, H., Okuya, M., Miyajima, A., Inukai, T., Funabiki, T., Endo, M., Look, A. T., and Kurosawa, H. (2004) *Blood* **103,** 3185–3191
6. Inaba, T., Inukai, T., Yoshihara, T., Seyshab, H., Ashmun, R. A., Canman, C. E., Laken, S. J., Kastan, M. B., and Look, A. T. (1996) *Nature* **382,** 541–544
7. Inukai, T., Inaba, T., Okushima, S., and Look, A. T. (1998) *Mol. Cell. Biol.* **18,** 6035–6043
8. Kinoshita, T., Yokota, T., Arai, K., and Miyajima, A. (1995) *EMBO J.* **14,** 266–275
9. Kuribara, R., Kinoshita, T., Miyajima, A., Shinjyo, T., Yoshihara, T., Inukai, T., Ozawa, K., Look, A. T., and Inaba, T. (1999) *Mol. Cell. Biol.* **19,** 2754–2762
10. Ikushima, S., Inukai, T., Inaba, T., Nimer, S. D., Cleveland, J. L., and Look, A. T. (1997) *Proc. Natl. Acad. Sci. U.S.A.* **94,** 2609–2614
11. Ambrosini, G., Adida, C., and Altieri, D. C. (1997) *Nat. Med.* **3,** 917–921
12. Sommer, K. W., Stumberger, C. J., Schmidt, G. E., Sasgary, S., and Cerni, C. (2003) *Oncogene* **22,** 4266–4280
13. Tamm, I., Wang, Y., Sausville, E., Scudiero, D. A., Vigne, N., Oltersdorf, T., and Reed, J. C. (1998) *Cancer Res.* **58,** 5315–5320
14. Li, F. (2003) *J. Cell. Physiol.* **197,** 8–29

15. Li, F., and Ling, X. (2006) *J. Cell. Physiol.* **208,** 476–486
16. Altieri, D. C. (2003) *Nat. Rev. Cancer* **3,** 46–54
17. Li, F., Ambrosini, G., Chu, E. Y., Plescia, J., Tognin, S., Marchisio, P. C., and Altieri, D. C. (1998) *Nature* **396,** 580–584
18. Li, F., and Altieri, D. C. (1999) *Biochem. J.* **344,** 305–311
19. Kurosawa, H., Goi, K., Inukai, T., Inaba, T., Chang, K. S., Shinjyo, T., Rake straw, K. M., Naeve, C. W., and Look, A. T. (1999) *Blood* **93,** 321–332
20. Kikuchi, J., Furukawa, Y., Iwase, S., Terui, Y., Nakamura, M., Kitagawa, S., Kitagawa, M., Komatsu, N., and Miura, Y. (1997) *Blood* **89,** 3980–3990
21. Rubinson, D. A., Dillon, C. P., Kwiatkowski, A. V., Sievers, C., Yang, L., Kopinja, J., Rooney, D. L., Zhang, M., Ihrig, M. M., McManus, M. T., Gertler, F. B., Scott, M. L., and Van Parijs, L. (2003) *Nat. Genet.* **33,** 401–406
22. Kikuchi, J., Shimizu, R., Wada, T., Ando, H., Nakamura, M., Ozawa, K., and Furukawa, Y. (2007) *Stem Cells* **25,** 2439–2447
23. Gu, C. M., Zhu, Y. K., Ma, Y. H., Zhang, M., Liao, B., Wu, H. Y., and Lin, H. L. (2006) *Neoplasm* **53,** 206–212
24. Inaba, T., Shapiro, L. H., Funabiki, T., Sinclair, A. E., Jones, B. G., Ashmun, R. A., and Look, A. T. (1994) *Mol. Cell. Biol.* **14,** 3403–3413
25. Kobayashi, K., Hatano, M., Otaki, M., Ogasawara, T., and Tokuhisa, T. (1999) *Proc. Natl. Acad. Sci. U.S.A.* **96,** 1457–1462
26. Deleted in proof
27. Moubarak, R. S., Yuste, V. J., Artus, C., Bouharrour, A., Greer, P. A., Menissier-de Murcia, J., and Susin, S. A. (2007) *Mol. Cell. Biol.* **27,** 4844–4862
28. Susin, S. A., Lorenzo, H. K., Zamzami, N., Marzo, I., Snow, B. E., Brothers, G. M., Mangion, J., Jacotot, E., Costantini, P., Loeffler, M., Larochette, N., Goodlett, D. R., Aebersold, R., Siderovski, D. P., Penninger, J. M., and Kroemer, G. (1999) *Nature* **397,** 441–446
29. Modjtahedi, N., Giordanetto, F., Madeo, F., and Kroemer, G. (2006) *Trends Cell Biol.* **16,** 264–272
30. Shinjyo, T., Kurosawa, H., Miyagi, J., Ohama, K., Masuda, M., Nagasaki, A., Matsui, H., Inaba, T., Furukawa, Y., and Takasu, N. (2008) *Tohoku J. Exp. Med.* **216,** 25–34
31. Carter, B. Z., Kornblau, S. M., Tsao, T., Wang, R. Y., Schober, W. D., Milella, M., Sung, H. G., Reed, J. C., and Andreeff, M. (2003) *Blood* **102,** 4179–4186
32. Liu, T., Brouha, B., and Grossman, D. (2004) *Oncogene* **23,** 39–48
33. Liu, T., Biddle, D., Hanks, A. N., Brouha, B., Yan, H., Lee, R. M., Leachman, S. A., and Grossman, D. (2006) *J. Invest. Dermatol.* **126,** 2247–2256
34. Croci, D. O., Cogno, I. S., Vittar, N. B., Salvatierra, E., Trajtenberg, F., Podhajcer, O. L., Osinaga, E., Rabinovich, G. A., and Rivarola, V. A. (2008) *J. Cell. Biochem.* **105,** 381–390
35. Yu, S. W., Wang, H., Poitras, M. F., Coombs, C., Bowers, W. J., Federoff, H. J., Poirier, G. G., Dawson, T. M., and Dawson, V. L. (2002) *Science* **297,** 259–263
36. Inukai, T., Inoue, A., Kurosawa, H., Goi, K., Shinjyo, T., Ozawa, K., Mao, M., Inaba, T., and Look, A. T. (1999) *Mol. Cell* **4,** 343–352
37. Metzstein, M. M., and Horvitz, H. R. (1999) *Mol. Cell* **4,** 309–319
38. Metzstein, M. M., Hengartner, M. O., Tsung, N., Ellis, R. E., and Horvitz, H. R. (1996) *Nature* **382,** 545–547
39. Inoue, A., Seidel, M. G., Wu, W., Kamizono, S., Ferrando, A. A., Bronson, R. T., Iwasaki, H., Akashi, K., Morimoto, A., Hitzler, J. K., Pestina, T. I., Jackson, C. W., Tanaka, R., Chong, M. J., McKinnon, P. J., Inukai, T., Grosveld, G. C., and Look, A. T. (2002) *Cancer Cell* **2,** 279–288
40. Tu, S. P., Jiang, X. H., Lin, M. C., Cui, J. T., Yang, Y., Lum, C. T., Zou, B., Zhu, Y. B., Jiang, S. H., Wong, W. M., Chan, A. O., Yuen, M. F., Lam, S. K., Kung, H. F., and Wong, B. C. (2003) *Cancer Res.* **63,** 7724–7732
41. Kanwar, J. R., Shen, W. P., Kanwar, R. K., Berg, R. W., and Krissansen, G. W. (2001) *J. Natl. Cancer Inst.* **93,** 1541–1552
42. Schimmer, A. D. (2004) *Cancer Res.* **64,** 7183–7190
43. Altieri, D. C. (2008) *Nat. Rev. Cancer* **8,** 61–70
44. Fukuda, S., and Pelus, L. M. (2006) *Mol. Cancer Ther.* **5,** 1087–1098

Ann Hematol
DOI 10.1007/s00277-009-0845-0

LETTER TO THE EDITOR

Idiopathic neutropenia with fewer than 5% dysplasia may be a distinct entity of idiopathic cytopenia of undetermined significance

Keiko Ando · Atsushi Kodama · Tamiko Iwabuchi · Junko H. Ohyashiki · Kazuma Ohyashiki

Received: 21 September 2009 / Accepted: 28 September 2009

Dear Editor,

A condition marked by fewer than 10% of dysplastic cells and fewer than 5% of blasts in the bone marrow (BM) is now categorized as idiopathic cytopenia of undetermined significance (ICUS); if clonal cytogenetic changes are detectable in ICUS patients, the diagnosis can be changed to myelodysplastic syndrome (MDS) [1]. This categorization is very practical and clear-cut in separating MDS from those with low-grade dysplasia [1], and it thus became possible to analyze the clinical and hematologic features to differentiate refractory cytopenia with unilineage dysplasia (RCUD) from ICUS. However, only a single report dealing with possible ICUS with dysplastic features in each cell lineage appears to exist, that by Wimazal et al. [2]. We therefore focused on cytopenia patients with fewer than 5% of BM blasts and reassessed the dysplastic features, in combination with the cytogenetic results, to shed light on low-grade dysplasia.

From 1994 to 2008, we performed BM examinations with cytogenetic studies in 445 patients with cytopenia, 237 of whom were given diagnoses of MDS or suspected MDS. As well as we could, we used the initial BM examination to rule out the possibility of other underlying disorders inducing cytopenia, and as a result, 137 patients with fewer than 5% marrow blasts were enrolled in this study. Of these 137 patients, 56 who were followed for more than 6 months and for whom specimens were available for reanalyzable marrow films (200 cells being examined in each cell lineage) were used in this study [3, 4]; two patients with hypoplastic BM without cytogenetic changes were excluded from this study since we could not completely rule out the possibility of low-grade aplastic anemia.

In this study, we reassessed the bone marrow films for 16 patients with ICUS (Electronic supplementary materials, File 1), 16 with RCUD (Electronic supplementary materials, File 2), and 22 patients with refractory cytopenia with multilineage dysplasia (RCMD; Electronic supplementary materials, File 3). No particular difference in the peripheral blood data was found among patients with ICUS, RCUD, and RCMD. RCUD patients had more dysgranulopoietic cells than those with ICUS (16.7± 19.4% vs 3.5±3.3%, P=0.0116) because of the presence of hypogranular neutrophils or pseudo-Pelger anomaly, while no significant difference in percentages of dyserythropoietic cells was noted (P=0.1809; Electronic supplementary materials, File 4). This indicates that ICUS patients can usually be diagnosed from the absence of prominent dysgranulopoiesis.

We then separated the ICUS patients into two groups according to the percentages of dysplastic cells (Table 1). ICUS patients with fewer than 5% dysplastic cells in at least one cell lineage had a significantly lower absolute neutrophil count than those with 5% to 9% of dysplastic

Electronic supplementary material The online version of this article (doi:10.1007/s00277-009-0845-0) contains supplementary material, which is available to authorized users.

K. Ando · T. Iwabuchi · K. Ohyashiki (✉)
The First Department of Internal Medicine (Hematology Division), Tokyo Medical University,
6-7-1 Nishishinjuku, Shinjuku-ku,
Tokyo 160-0023, Japan
e-mail: ohyashik@rr.iij4u.or.jp

A. Kodama
Division of Cytogenetics, Central Laboratory,
Tokyo Medical University,
Tokyo, Japan

J. H. Ohyashiki
Intractable Disease Research Center, Tokyo Medical University,
Tokyo, Japan

Published online: 13 October 2009

Table 1 Hematologic parameters of patients with idiopathic cytopenia of undetermined significance classified by percentages of dysplastic cells

	ICUS (<5% dysplasia)	ICUS (5–9% dysplasia)	*P* value
No. of patients	7	9	
Age (years)	55.6±14.9	53.0±20.7	0.7861
Leukocytes ($\times 10^6$/L)	2,586±647	3,533±1,587	0.1616
Neutrophils ($\times 10^6$/L)	1,086±296	2,308±1,305	0.0302
Lymphocytes ($\times 10^6$/L)	1,273±421	1,016±310	0.1815
Monocytes ($\times 10^6$/L)	117±53	184±137	0.2429
Hb (g/dL)	12.4±1.9	11.4±3.4	0.5172
Platelets ($\times 10^9$/L)	197±78	111±94	0.071
MCV (fL)	94.8±5.8	98.6±15.0	0.5386
Marrow blasts (%)	1.6±0.6	1.9±1.2	0.5864
Dyserythropoiesis (%)	1.4±1.1	3.4±2.8	0.0994
Dysgranulopoiesis (%)	1.4±1.2	5.1±3.5	0.0176
Cytogenetics			
Normal karyotypes	7	6	
Non-clonal changes	0	0	
Clonal changes	0	3 (2*)	

Hb hemoglobin, *MCV* mean corpuscular volume, 2* two patients showed a clonal missing Y chromosome

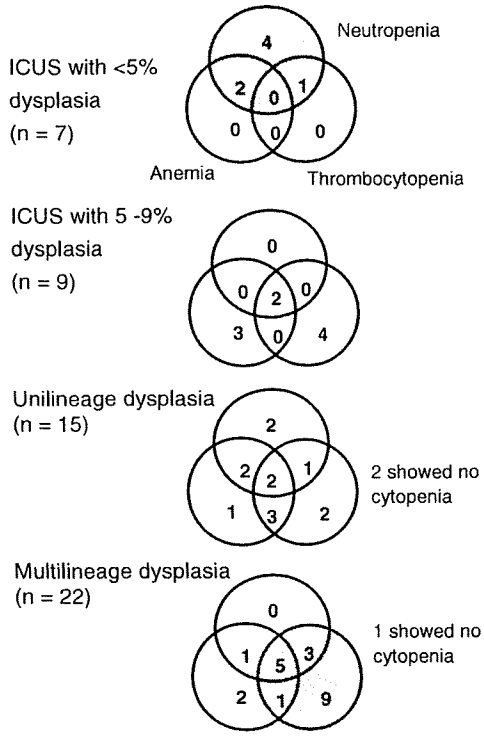

Fig. 1 Diagram of cytopenia pattern in patients showing fewer than 5% of marrow blasts. Overlapping portions show cytopenia in two cell lineages (bi-cytopenia), and the central overlapping portion indicates pancytopenia. Note the cytopenic pattern in the ICUS patients with <5% dysplasia (*top*) who show predominant neutropenia. One RARS patient with unilineage dysplasia is excluded from this diagram. We utilized the definition of the Working Conference on MDS for cytopenia [4]; neutropenia for less than $1,500\times10^6$/L, hemoglobin for less than 11 g/dL, and thrombocytopenia for less than 100×10^9/L

cells ($1,086\pm296\times10^6$/L vs $2,308\pm1,305\times10^6$/L; $P=0.0302$), while the leukocyte counts did not differ significantly: $2,586\pm647\times10^6$/L vs $3,533\pm1,587\times10^6$/L ($P=0.1616$). The pattern of cytopenia in the ICUS patients with fewer than 5% dysplastic cells showed prominent neutropenia (less than $1,500\times10^6$/L; Fig. 1). Chromosome changes were detected in only three patients with ICUS with 5% to 9% of dysplastic cells: One showed non-clonal del(20q) and −Y, one, −Y, and one clonal del(20q). None of them developed MDS or aplastic anemia during a mean follow-up period of 42.25 months.

The current observation indicates that ICUS patients may be heterogeneous and that the group with fewer dysplastic cells with no detectable cytogenetic changes preferentially exhibited neutropenia (Fig. 1), and so the etiology of patients in this group may be different from the ICUS patients with more dysplastic cells (5% to 9%). Another point that was noticed is that all three patients (two with ICUS morphology and one with RCUD) with del (20q), whether they had a clonal nature or not, consistently exhibited thrombocytopenia alone and were clustered in the low blast percentage and low dysplastic cell frequency group. This suggests that the detection of cells with del (20q), using fluorescence in situ hybridization analysis, in low-grade MDS, including morphologically identified ICUS [5], might be important in MDS diagnosis since the detection of cytogenetic changes is important in the diagnosis of MDS.

Acknowledgments Thanks are due to Professor J Patrick Barron, of the International Medical Communication Center of Tokyo Medical University, for his review of this manuscript. AK, TI, and KO

performed hematologic examination, AK did cytogenetic study, and JHO reviewed the paper.

Conflict of interest None.

References

1. Brunning RD, Orazi A, Germing U, Le Beau MM, Porwit A, Vardiman JW et al (2008) Myelodysplastic syndromes. In: Swerdlow SH, Campo E, Harris NL, Jaffe ES, Pileri SA, Stein H, Thiele J, Vardiman JW (eds) WHO classification of tumours of hematopoietic and lymphoid tissues. IARC, Lyon, pp 90–107
2. Wimazal F, Fonatsch C, Thalhammer R, Schwarzinger I, Müllauer L, Sperr WR et al (2007) Idiopathic cytopenia of undetermined significance (ICUS) versus low risk MDS: the diagnostic interface. Leuk Res 31:1461–1468
3. Mufti GJ, Bennett JM, Goasguen J, Bain BJ, Baumann I, Brunning R, International Working Group on Morphology of Myelodysplastic Syndrome et al (2008) Diagnosis and classification of myelodysplastic syndrome: International Working Group on Morphology of myelodysplastic syndrome (IWGM-MDS) consensus proposals for the definition and enumeration of myeloblasts and ring sideroblasts. Haematologica 93:1712–1717
4. Valent P, Horney H-P, Bennett JM, Fonatsch C, Germing U, Greenberg P et al (2007) Definitions and standards in the diagnosis and treatment of the myelodysplastic syndromes: consensus statements and report from a working conference. Leuk Res 31:727–736
5. Gupta R, Soupir CP, Johari V, Hasserjian RP (2007) Myelodysplastic syndrome with isolated deletion of chromosome 20q: an indolent disease with minimal morphological dysplasia and frequent thrombocytopenic presentation. Br J Haematol 139:265–288

Oncogene (2010), 1–13

www.nature.com/onc

ORIGINAL ARTICLE

Identification of *Zfp521/ZNF521* as a cooperative gene for *E2A-HLF* to develop acute B-lineage leukemia

N Yamasaki[1], K Miyazaki[1], A Nagamachi[2], R Koller[3], H Oda[4], M Miyazaki[5], T Sasaki[1], Z-i Honda[6], L Wolff[3], T Inaba[2] and H Honda[1]

[1]*Department of Developmental Biology, Research Institute for Radiation Biology and Medicine, Hiroshima University, Minami-ku, Hiroshima, Japan;* [2]*Department of Molecular Oncology, Research Institute for Radiation Biology and Medicine, Hiroshima University, Minami-ku, Hiroshima, Japan;* [3]*Leukemogenosis Section, Laboratory of Cellular Oncology, National Cancer Institute, NIH, Bethesda, MD, USA;* [4]*Department of Pathology, Tokyo Women's Medical University, Shinjuku-ku, Tokyo, Japan;* [5]*Department of Immunology, Graduate School of Biomedical Sciences, Hiroshima University, Minami-ku, Hiroshima, Japan and* [6]*Department of Allergy and Rheumatology, Faculty of Medicine, Graduate School of Medicine, University of Tokyo, Bunkyo-ku, Tokyo, Japan*

E2A-hepatic leukemia factor (HLF) is a chimeric protein found in B-lineage acute lymphoblastic leukemia (ALL) with t(17;19). To analyze the leukemogenic process and to create model mice for t(17;19)-positive leukemia, we generated inducible knock-in (iKI) mice for *E2A-HLF*. Despite the induced expression of *E2A-HLF* in the hematopoietic tissues, no disease was developed during the long observation period, indicating that additional gene alterations are required to develop leukemia. To elucidate this process, *E2A-HLF* iKI and control littermates were subjected to retroviral insertional mutagenesis. Virus infection induced acute leukemias in *E2A-HLF* iKI mice with higher morbidity and mortality than in control mice. Inverse PCR detected three common integration sites specific for *E2A-HLF* iKI leukemic mice, which induced overexpression of zinc-finger transcription factors: *growth factor independent 1* (*Gfi1*), *zinc-finger protein subfamily 1A1 isoform a* (*Zfp1a1*, also known as *Ikaros*) and *zinc-finger protein 521* (*Zfp521*). Interestingly, tumors with *Zfp521* integration exclusively showed B-lineage ALL, which corresponds to the phenotype of human t(17;19)-positive leukemia. In addition, *ZNF521* (human counterpart of *Zfp521*) was found to be overexpressed in human leukemic cell lines harboring t(17;19). Moreover, both iKI for *E2A-HLF* and transgenic for *Zfp521* mice frequently developed B-lineage ALL. These results indicate that a set of transcription factors promote leukemic transformation of *E2A-HLF*-expressing hematopoietic progenitors and suggest that aberrant expression of *Zfp521/ZNF521* may be clinically relevant to t(17;19)-positive B-lineage ALL.

Oncogene advance online publication, 11 January 2010; doi:10.1038/onc.2009.475

Keywords: *E2A-HLF*; inducible knock-in mice; retrovirus insertional mutagenesis; *Zfp521/ZNF521*

Correspondence: Dr H Honda, Department of Developmental Biology, Research Institute for Radiation Biology and Medicine, 1-2-3, Kasumi, Minami-ku, Hiroshima 734-8553, Japan.
E-mail: hhonda@hiroshima-u.ac.jp
Received 5 May 2009; revised 16 July 2009; accepted 23 November 2009

Introduction

The *E2A* gene, which encodes a basic helix-loop-helix transcription factor of E-box DNA-binding proteins on chromosome 19, is the target of subsets of B-lineage acute lymphoblastic leukemia (ALL) (Look, 1997). As a result of the t(17;19)(q22;p13), the *E2A* gene is fused to the *HLF* gene on chromosome 17 (Inaba *et al.*, 1992). In the *E2A-HLF* chimeric gene product, the transactivation domain of E2A is fused to the basic region/leucine zipper domain of hepatic leukemia factor (HLF), which contributes to the DNA binding and dimerization (Inaba *et al.*, 1992). Clinically, ALL with the E2A-HLF chimera is refractory to intensive therapy and is frequently associated with coagulopathy and hypercalcemia (Hunger, 1996).

The biological properties of E2A-HLF were initially analyzed using cultured cells. We showed that the expression of *E2A-HLF* in NIH 3T3 cells induced anchorage-independent cell growth in soft agar and rendered these cells tumorigenic in nude mice (Yoshihara *et al.*, 1995; Inukai *et al.*, 1997). In addition, using a zinc-inducible system, we showed that *E2A-HLF* expression protects interleukin 3-dependent hematopoietic cells from interleukin 3 deprivation-induced apoptosis (Inaba *et al.*, 1996). Moreover, by a representational difference analysis, several downstream candidate genes of *E2A-HLF* were cloned, such as *annexin II* (Matsunaga *et al.*, 2003), *annexin VIII* and *sushi-repeat protein upregulated in leukemia* (*SRPUL*; Kurosawa *et al.*, 1999), two *Groucho*-related genes, *Grg2* and *Grg6* (Dang *et al.*, 2001), and a gene encoding a zinc-finger transcription factor, *Slug* (Inukai *et al.*, 1999).

The *in vivo* roles of *E2A-HLF* were analyzed by transgenic and bone marrow transplantation studies. We and others generated transgenic mice expressing *E2A-HLF* under the control of lymphoid-specific promoters (Honda *et al.*, 1999; Smith *et al.*, 1999). The transgenic mice showed increased thymocyte apoptosis, B-cell maturation arrest and eventual development of ALL, mainly with T-cell phenotype (Honda *et al.*, 1999; Smith *et al.*, 1999). On the other hand, bone marrow (BM) B-cell progenitors retrovirally co-transduced

with *E2A-HLF* and *Bcl-2* produced immortalized cells, which developed leukemia when transplanted into syngeneic recipients (Smith *et al.*, 2002). These results showed that the expression of *E2A-HLF* perturbed normal lymphocyte development, rendered lymphocytes susceptible to malignant transformation and finally developed ALL. Interestingly, the phenotypes of the *E2A-HLF* transgenic mice closely resembled those of *E2A*-deficient mice, which also showed abnormal T-cell development, absence of B-cell precursors and rapid development of T-cell lymphomas (Bain *et al.*, 1994, 1997; Zhuang *et al.*, 1994). These results strongly suggested that *E2A-HLF* contributes to leukemogenesis by activating downstream target genes and/or by suppressing transcriptional activity of endogenous genes in a dominant-negative manner (Aspland *et al.*, 2001; Seidel and Look, 2001).

We showed the *in vivo* oncogenecity of *E2A-HLF* by a transgenic approach (Honda *et al.*, 1999). However, the transgenic system fundamentally differs from human disease in several ways. First, in the transgenic system, every cell contains the transgene and there are no normal cells, whereas the human disease originates from acquiredly transformed cells. Second, in the transgenic system, as the transgene-derived product is congenitally expressed, transgene-expressing cells are not eliminated by the immune system. In contrast, in human diseases, most transformed cells are ablated by immunocompetent cell and those that escape from this system proliferate and show a fully malignant phenotype. Therefore, the precise molecular mechanism(s) through which *E2A-HLF* contributes a growth advantage to hematopoietic cells and develops leukemia *in vivo* remains to be clarified.

In this study we report the generation and analysis of knock-in mice for *E2A-HLF* in which *E2A-HLF* was inducibly expressed under the control of the native regulatory elements of the *E2A* gene. Despite the induced *E2A-HLF* expression in the hematopoietic tissues, no disease was developed during the long-term observation period, indicating that secondary events are required for the development of leukemia. To elucidate this process, we applied retroviral insertional mutagenesis (RIM) using Moloney murine leukemia virus (MMLV), isolated common viral integration sites specific for *E2A-HLF*-expressing tumors, and identified *Zfp521/ZNF521* as a cooperative gene for *E2A-HLF* to develop B-lineage ALL.

Results

Generation of inducible knock-in (iKI) mice for E2A-HLF *and acquired expression of E2A-HLF in the hematopoietic tissues*

To study the role of *E2A-HLF* in model animal systems that mimic human leukemogenesis, we planned to generate mice in which *E2A-HLF* could be inducibly expressed under the control of the native *E2A* promoter. For this purpose, we designed a knock-in vector in which a genomic region of the *E2A* gene (a 3′ part of exon 2, intron 2 and a 5′ part of exon 3) was replaced by a cassette containing the *floxed neomycin* resistance (*Neo*) gene, followed by *E2A-HLF* complementary DNA, *IRES-GFP* (*IG*) and an *SV40 polyA* signal (*pA*) (Figure 1a). Embryonic stem cell clones with homologous recombination were identified by Southern blot analysis (Figure 1b, upper panel) using a 5′ probe (Figure 1a) and by long-distance genomic PCR (Figure 1b, lower panel) using a 3′ primer set (*P1* and *P2*, Figure 1a) and were used to create chimeric mice, which transmitted the mutant allele to the progeny and produced heterozygous mice ($EHKI^{Neo+}$). In the $EHKI^{Neo+}$ mice, the expression of the knock-in allele-derived message was detected by reverse transcriptase–PCR (RT–PCR) using a primer set, *E2A-77* (derived from exon 1 of the *E2A* gene) and *HLF-2* (derived from the *HLF* portion of the *E2A-HLF* fusion complementary DNA) (Figure 1a) in all tissues examined (indicated by *Neo*+ in Figure 1c, upper panel). However, because this message contains a *floxed Neo* gene and multiple in-frame stop codons, the E2A-HLF fusion protein cannot be translated. To confirm this, proteins extracted from tissues were immunoprecipitated with an anti-E2A antibody and immunoprecipitants were blotted with an anti-HLF antibody. As expected, no E2A-HLF protein (molecular weight 62 kDa) was detected in the hematopoietic tissues, such as the thymus or spleen of $EHKI^{Neo+}$ mice (the first and fourth lanes in Figure 1d).

We then mated $EHKI^{Neo+}$ mice with *MxCre* transgenic mice that express *Cre* under the control of the interferon-responsive *Mx* promoter (Kuhn *et al.*, 1995). $EHKI^{Neo+}/MxCre$ compound mice were injected with polyinosinic/polycytidylic acid (pIpC), which is a strong and transient inducer of interferon, to delete the *floxed Neo* gene from the knocked-in allele and to create *Neo*-deleted ($EHKI^{\Delta Neo}$) mice (Figure 1a). In the pIpC-treated $EHKI^{Neo+}/MxCre$ (that is, $EHKI^{\Delta Neo}$) mice, a shorter message was amplified in various tissues, including the thymus, heart, liver and spleen, by RT–PCR using *E2A-77* and *HLF-2* primers (indicated by Δ*Neo* in Figure 1c, lower panel), indicating that the *Neo* gene was successfully deleted in these tissues. As a result, the induced expression of E2A-HLF protein was achieved, as shown by immunoprecipitation/western blot analysis in the thymus and spleen of the $EHKI^{\Delta Neo}$ mice (the second and fifth lanes in Figure 1d).

MMLV infection induced acute leukemias in $EHKI^{\Delta Neo}$ *mice at a higher frequency and with a shorter latency than in* $EHKI^{Neo+}$ *mice*

$EHKI^{Neo+}$ and $EHKI^{Neo+}/MxCre$ mice treated with pIpC were continuously observed for any sign of illness, including routine examination of peripheral blood parameters. However, during the long-term observation period, no abnormality was detected in $EHKI^{Neo+}$ or $EHKI^{\Delta Neo}$ mice (Figure 2a, thin dotted and thin continuous lines). These results indicated that the induced *E2A-HLF* expression alone is not sufficient

and additional genetic changes are required for the development of leukemia.

To address this possibility, mice were subjected to retroviral insertional mutagenesis. Neonatal *EHKI*$^{Neo+}$ and *EHKI*$^{Neo+}$*/MxCre* mice were infected with MMLV and were then injected with pIpC. Both types of mice developed leukemias, but MMLV-infected *EHKI*$^{\Delta Neo}$ (*EHKI*$^{\Delta Neo}$/MMLV) mice showed higher morbidity and mortality than virus-infected *EHKI*$^{Neo+}$ (*EHKI*$^{Neo+}$/MMLV) littermates (Figure 2a, thick dotted and thick continuous lines). *EHKI*$^{\Delta Neo}$/MMLV mice began to develop acute leukemias at as early as 2.6 months of age, and all died by 6 months of age. In contrast, *EHKI*$^{Neo+}$/MMLV mice developed leukemias at approximately 4–6 months of age and 6 out of 11 mice died within 1 year. The difference in the survival curves between *EHKI*$^{\Delta Neo}$/MMLV and *EHKI*$^{Neo+}$/MMLV mice was statistically significant ($P<0.01$).

EHKI^{Neo+}*/MMLV mice mainly developed T-cell leukemia but* EHKI$^{\Delta Neo}$*/MMLV mice showed B-progenitor and lineage marker-negative leukemias*

The leukemic mice were hematologically and macroscopically examined, and the leukemic cells were immunophenotypically and molecularly analyzed. Interestingly, macroscopic appearances of *EHKI*$^{Neo+}$/MMLV leukemic mice were different from those of *EHKI*$^{\Delta Neo}$/MMLV leukemic mice.

Most of *EHKI*$^{Neo+}$/MMLV leukemic mice (four of six samples) showed thymic enlargement, associated with splenomegaly and lymph node swelling, except two

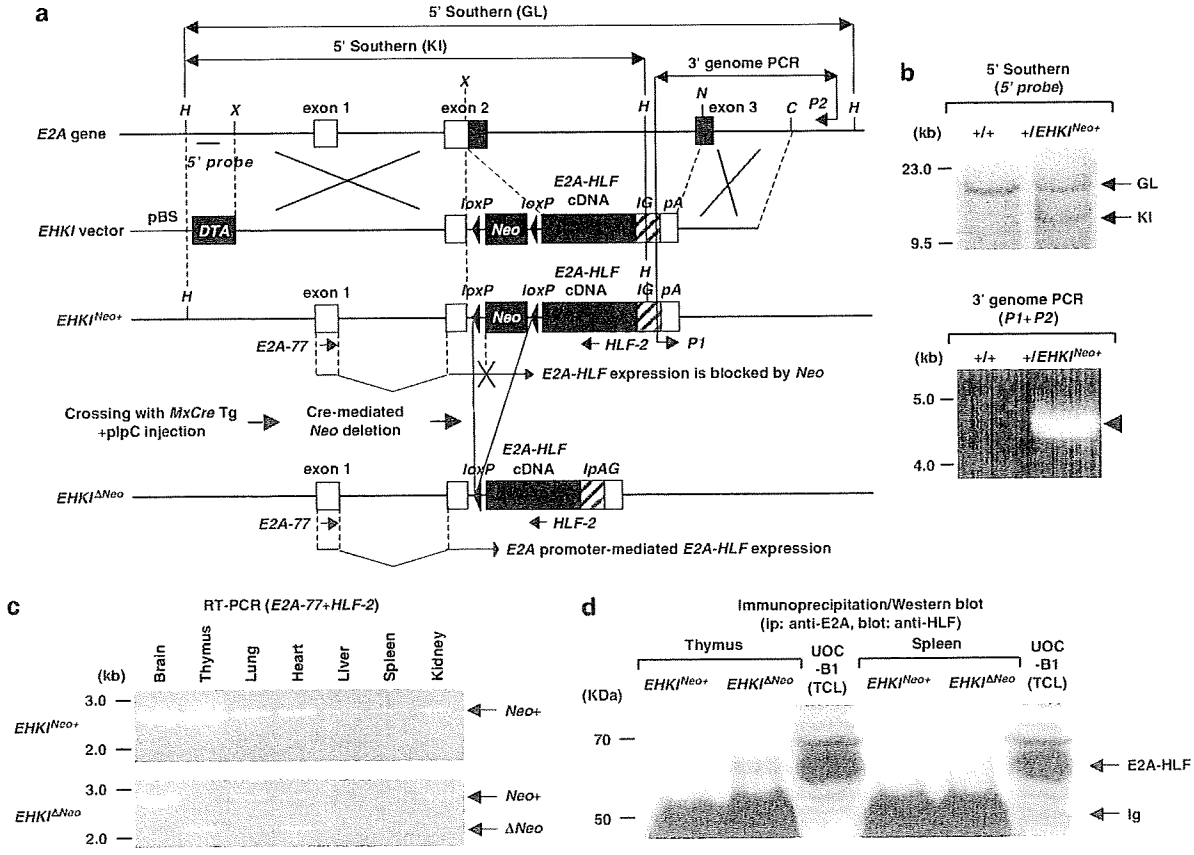

Figure 1 Generation of inducible knock-in (iKI) mice for *E2A-HLF* and the acquired expression of E2A-HLF in the hematopoietic tissues. (**a**) Schematic illustration of the iKI strategy. Part of the non-coding region of exon 2, the coding region of exon 2, intron 2 and part of the coding region of exon 3 were replaced with the *floxed neomycin* resistance gene, followed by *E2A-HLF* fusion complementary (cDNA), *IRES-GFP* (*IG*) and a *polyadenylation* signal (*pA*). Restriction enzymes: *H*, *Hind*III; *X*, *Xba*I; *N*; *Nae*I; *C*;, *Cla*I. The positions of the 5′ probe for Southern blot analysis, *P1* and *P2* primers for genomic PCR and *E2A-77* and *HLF-2* for RT–PCR are shown. (**b**) Results of 5′ Southern blot analysis and 3′ genomic PCR to detect homologous recombination. Positions of germline (GL)- and KI-allele-derived bands determined by 5′ Southern blot analysis are indicated by arrows (upper panel) and the PCR product generated by 3′ genomic PCR is indicated by an arrowhead (lower panel). (**c**) Expression of the KI allele-derived mRNA. mRNAs extracted from tissues of *EHKI*$^{Neo+}$ and *EHKI*$^{\Delta Neo}$ mice were subjected to RT–PCR using *E2A-77* and *HLF-2* primers (seea). Positions of RT–PCR products with and without *Neo* are indicated by *Neo*+ and Δ*Neo*, respectively. (**d**) Acquired E2A-HLF protein expression in the lymphoid tissues of *EHKI*$^{\Delta Neo}$ mice. Proteins extracted from the thymus and spleen were immunoprecipitated with an anti-E2A antibody, and the immunoprecipitants were blotted with an anti-HLF antibody. The positions of E2A-HLF protein and immunoglobulin (Ig) are indicated by arrows. Total cell lysate (TCL) from a t(17;19)$^{+}$ cell line, UOCB1, was used as a positive control.

samples that showed splenomegaly and lymph node swelling. In contrast, *EHKI*$^{\Delta Neo}$/MMLV leukemic mice did not show thymic enlargement but showed splenomegaly, frequently associated with lymph node swelling. To determine the lineage of the leukemic cells, disaggregated cells were subjected to flow cytometric analysis. In *EHKI*$^{Neo+}$/MMLV mice, samples with thymic enlargement (nos. 1 and 3–5) were positive for T-cell (Thy1.2) antigen, but negative for B-cell (B220), myeloid (Gr1) and macrophage (Mac1) antigens, whereas the other two samples lacking thymic enlargement (nos. 2 and 6) did not express any of Thy1.2, B220, Gr1 or Mac1 antigen. In *EHKI*$^{\Delta Neo}$/MMLV mice, two samples (nos. 2 and 4) were positive

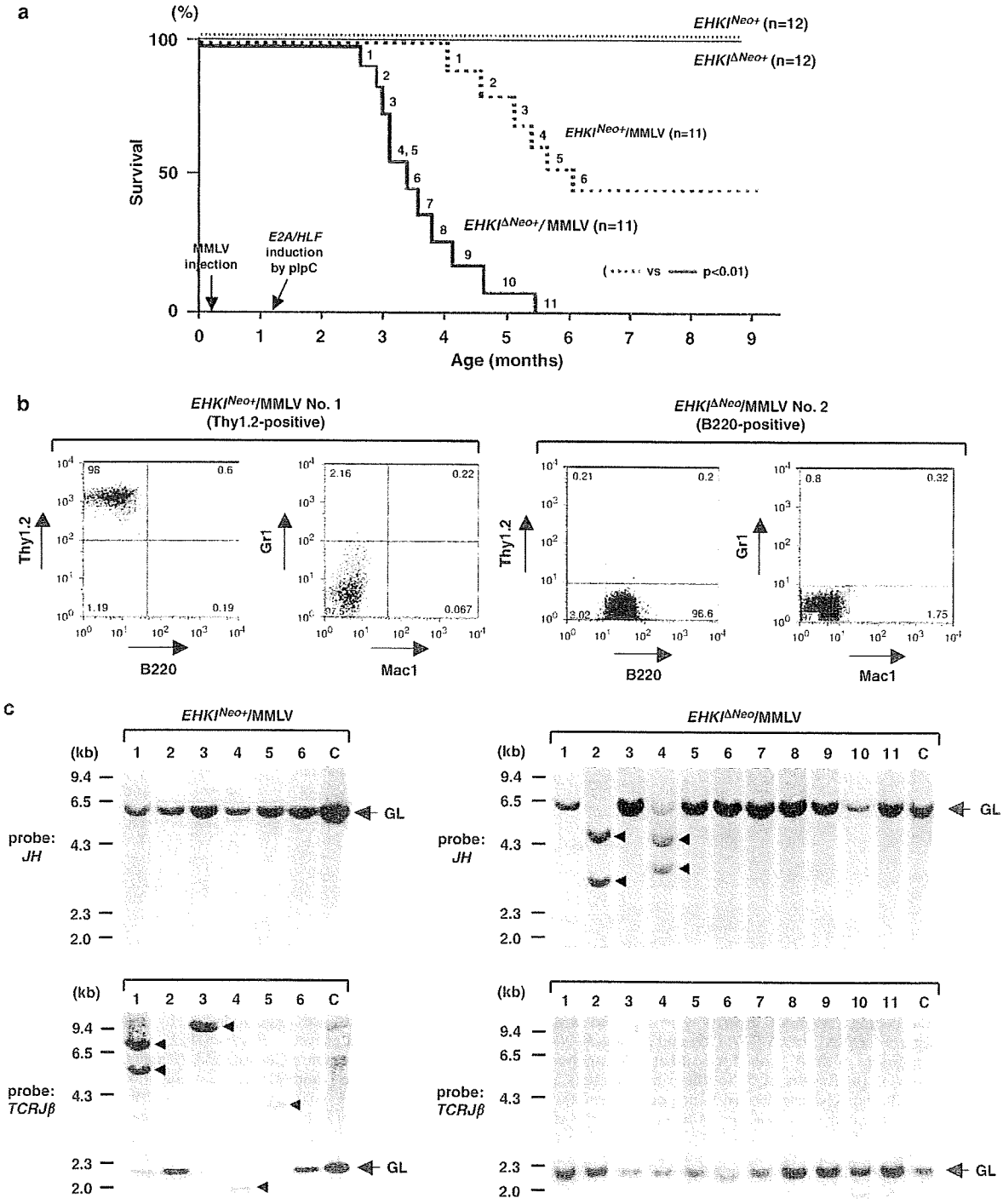

for B220 but negative for other antigens, whereas the remaining 9 samples (nos. 1, 3 and 5–11) did not express any of Thy1.2, B220, Gr1 or Mac1 antigen. Representative results of flow cytometric analysis of Thy1.2-positive *EHKI*$^{Neo+}$/MMLV leukemic samples and B220-positive *EHKI*$^{\Delta Neo}$/MMLV leukemic samples are shown in Figure 2b. As B-lineage leukemia is rarely developed in MMLV-infected mice, B-cell commitment of the two B220-positive samples (nos. 2 and 4 of *EHKI*$^{\Delta Neo}$/MMLV mice) was further analyzed by using antibodies against CD19, BP1, CD20, CD43 and immunoglobulin M. The result showed that both samples were positive for CD19, BP1, CD20 and CD43 but negative for immunoglobulin M, showing that they were B-progenitor leukemias (Supplementary Figure 1).

The leukemic samples were then subjected to gene rearrangement analysis using *JH* and *TCRJ-β* probes. As expected from the results of flow cytometric analyses, Thy1.2-positive samples (nos. 1 and 3–5 of *EHKI*$^{Neo+}$/MMLV group) showed rearranged bands in the *TCR-β* locus (indicated by arrowheads in the left lower panel of Figure 2c), and B220-positive samples (No. 2 and 4 of *EHKI*$^{\Delta Neo}$/MMLV group) showed rearranged bands in the *IgH* locus (indicated by arrowheads in the right upper panel of Figure 2c), whereas other samples lacking lineage markers (nos. 2 and 6 of *EHKI*$^{Neo+}$/MMLV mice and nos. 1, 3, and 5–11 of *EHKI*$^{\Delta Neo}$/MMLV mice) showed germline patterns in both *IgH* and *TCR-β* regions. These results indicated that four *EHKI*$^{Neo+}$/MMLV leukemias (nos. 1 and 3∼5) were T-cell ALL and two *EHKI*$^{\Delta Neo}$/MMLV leukemias (nos. 2 and 4) were B-lineage ALL, but others were lineage marker-negative leukemias that were derived from immature cells not yet committed to a specific cell lineage. The characteristics of *EHKI*$^{Neo+}$/MMLV and *EHKI*$^{\Delta Neo}$/MMLV leukemic mice are summarized in Table 1.

Identification of Gfi1, Ikaros *and* Zfp521 *as common integration sites (CISs) in leukemias developed in* EHKI$^{\Delta Neo}$/*MMLV mice*

To identify gene(s) whose altered expression cooperated with *E2A-HLF*, genomic DNAs extracted from leukemic samples of *EHKI*$^{\Delta Neo}$/MMLV mice were subjected to inverse PCR (iPCR). DNAs from leukemias of *EHKI*$^{Neo+}$/MMLV mice were also analyzed as controls. Genes identified by iPCR in *EHKI*$^{\Delta Neo}$/MMLV and *EHKI*$^{Neo+}$/MMLV leukemic mice are listed in Supplementary Tables 1 and 2, respectively. In the iPCR products of *EHKI*$^{\Delta Neo}$/MMLV mice, we found three CISs (shown by asterisks and bold type in Supplementary Table 1), all of which encode zinc-finger transcription factors.

First, in four leukemic samples (nos. 1, 6, 8 and 11), viruses were integrated in an ∼10-kb upstream region (nos. 1, 8 and 11) or in the 3′ untranslated region (no. 6) of *growth factor independent 1* (*Gfi1*) gene (upper panel of Figure 3a). Southern blot analysis using genomic fragments adjacent to the integration sites showed rearrangement bands in all the tumors (indicated by arrowheads in the lower left panel of Figure 3a), indicating that cells with these integration sites were predominant in the related tumors. In addition, northern blot analysis revealed that *Gfi1* mRNA expression levels were significantly enhanced in nos. 1, 8 and 11, and moderately increased in no. 6 when compared with those in a control spleen (C) and *Gfi1*-non-integrated samples (nos. 7 and 10, see Table 1 and Supplementary Table 1) (indicated by an arrow in the lower right panel of Figure 3a).

Second, *zinc-finger protein subfamily 1A1 isoform a* (*Zfp1a1*, also known as *Ikaros*, hereafter referred to as *Ikaros*) gene was the retroviral target in three samples (nos. 3, 5 and 9). Integrations occurred in intron 1 (nos. 3 and 5) and intron 3 (no. 9) (upper panel of Figure 3b). All these three samples (nos. 3, 5 and 9) carried rearranged bands (indicated by arrowheads in the lower left panel of Figure 3b) and showed enhanced *Ikaros* mRNA expression when compared with a control spleen (C) and *Ikaros*-non-integrated samples (nos. 7 and 10) (indicated by an arrow in the lower middle panel of Figure 3b). Previous reports showed that Ikaros contributes to leukemogenesis by an isoform change from normally expressed forms (Ikaros (Ik)-1, Ik-2, Ik-3 and Ik-4) to a shorter splicing variant, Ik-6, which suppresses downstream gene expressions in a dominant-negative manner (Nakayama *et al*., 1999; Beverly and Capobianco, 2003). To analyze whether *Ik-6* mRNA was expressed in the three *Ikaros*-integrated samples, we performed RT–PCR to detect alternatively spliced mRNA isoforms. All three samples expressed *Ik-1, -2, -3* and *-4* mRNAs but did not express *Ik-6* mRNA (lower right panel of Figure 3b), indicating that the viral integrations simply upregulated *Ikaros* gene expression without affecting splicing.

Figure 2 Survival curves of *EHKI*$^{Neo+}$ and *EHKI*$^{\Delta Neo}$ mice with or without MMLV infection, and flow cytometric and gene rearrangement analyses of leukemic tissues of *EHKI*$^{Neo+}$ and *EHKI*$^{\Delta Neo}$ mice infected with MMLV (*EHKI*$^{Neo+}$/MMLV and *EHKI*$^{\Delta Neo}$/MMLV). (**a**) Survival curves of *EHKI*$^{Neo+}$, *EHKI*$^{\Delta Neo}$, *EHKI*$^{Neo+}$/MMLV and *EHKI*$^{\Delta Neo}$/MMLV mice. No disease was observed in *EHKI*$^{Neo+}$ or *EHKI*$^{\Delta Neo}$ mice (indicated by thin dotted and thin continuous lines, respectively). MMLV infection induced acute leukemias in both *EHKI*$^{Neo+}$/MMLV and *EHKI*$^{\Delta Neo}$/MMLV mice (indicated by thick dotted and thick continuous lines, respectively) and the *EHKI*$^{\Delta Neo}$/MMLV mice showed higher morbidity and mortality than *EHKI*$^{Neo+}$/MMLV mice. The diseased *EHKI*$^{\Delta Neo}$/MMLV and *EHKI*$^{Neo+}$/MMLV mice are numbered and the time points of MMLV injection and *E2A-HLF* induction by pIpC are indicated by arrows. (**b**) Representative results of a flow cytometric analysis. Leukemic cells in *EHKI*$^{Neo+}$/MMLV and *EHKI*$^{\Delta Neo}$/MMLV mice were stained with anti-Thy1.2, anti-B220, anti-Gr1 and anti-Mac1 antibodies and analyzed using a FACSCalibur. No. 1 of *EHKI*$^{Neo+}$/MMLV leukemic mice that was positive for Thy1.2 but negative for other antigens and no. 2 of *EHKI*$^{\Delta Neo}$/MMLV leukemic mice that was positive for B220 but was negative for other antigens are shown in the left and right panels, respectively. (**c**) Results of gene rearrangement analysis. DNAs extracted from leukemic tissues of *EHKI*$^{Neo+}$/MMLV and *EHKI*$^{\Delta Neo}$/MMLV mice were digested with *Eco*RI and blotted with *JH* (upper panels) and *TCRJ-β* (lower panels) probes. Germline (GL) and rearranged bands are indicated by arrows and arrowheads, respectively.

Finally, *zinc-finger protein 521) (Zfp521,* also known as *Evi3*) gene was integrated by retroviruses in two B-lineage leukemia mice (nos. 2 and 4). One integration site was in the 5′ upstream region and the other was in the 5′ untranslated region of exon 1 (upper panel of Figure 3c). Both samples showed rearranged gene patterns (indicated by arrowheads in the lower left panel of Figure 3c) and showed enhanced *Zfp521* mRNA expression when compared with a control spleen (C) and *Zfp521*-non-integrated samples (nos. 7 and 10) (indicated by arrows in the lower right panel of Figure 3c).

On the other hand, among the iPCR products of *EHKI*$^{Neo+}$/MMLV leukemic mice, we detected one CIS, which was *Abelson helper integration site 1* (*Ahi1*) gene (shown by asterisks and bold type in Supplementary Table 2). This CIS was found in samples 3 and 4, in which retroviruses were integrated in introns 9 and 23,

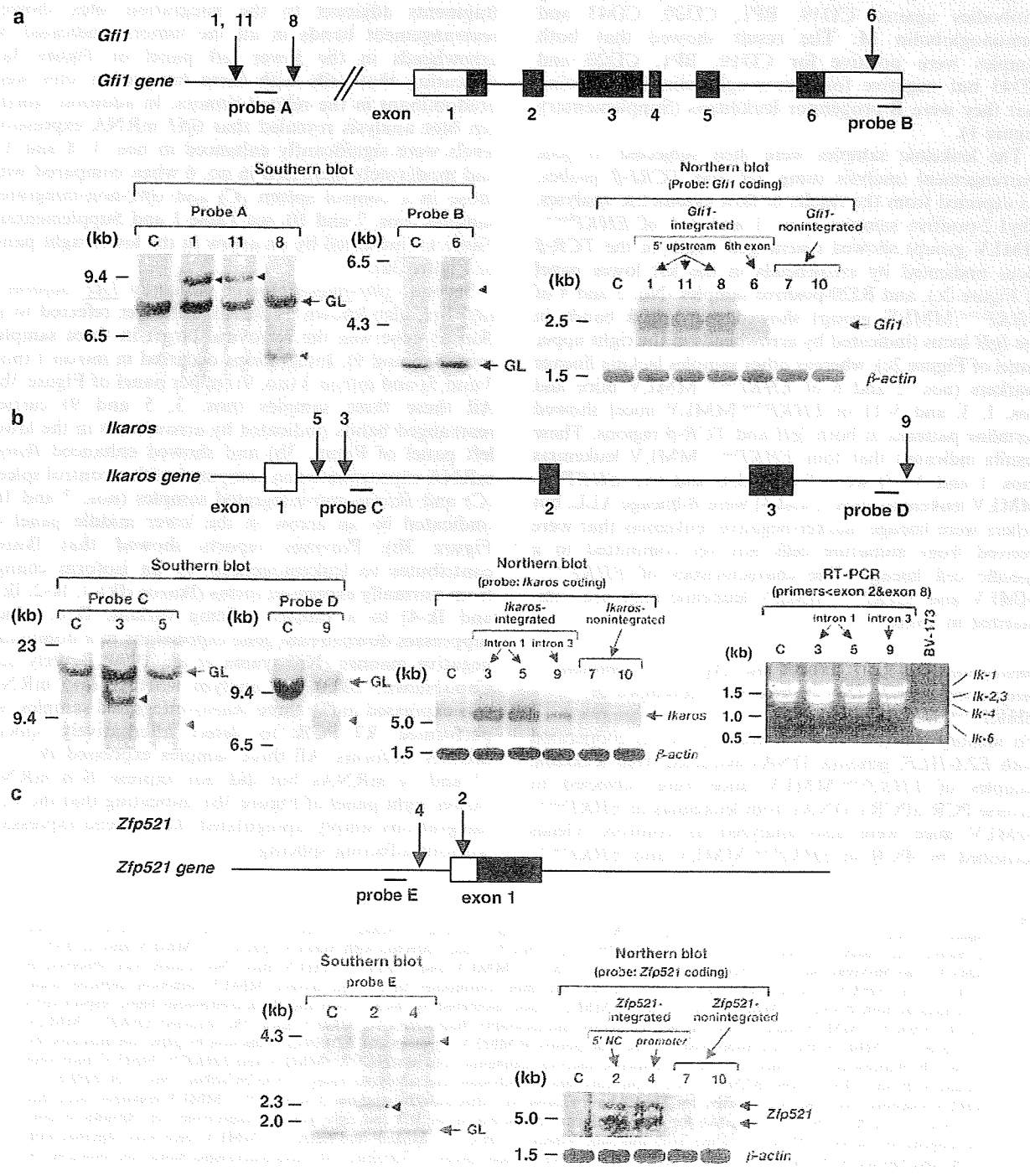

respectively (upper panel of Supplementary Figure 2). Southern blot analyses using genomic fragments adjacent to the integration sites detected rearranged bands, indicating that these are the major integration sites in the related tumors (indicated by arrowheads in the lower panel of Supplementary Figure 2).

Taken together, the iPCR analysis revealed that the virus integrations in three transcription factors, *Gfi1*, *Ikaros* and *Zfp521*, were preferentially associated with *EHKI*$^{\Delta Neo}$/MMLV leukemias and strongly suggested that overexpression and/or aberrant expression of these gene products would have a cooperative role with *E2A-HLF* in the leukemogenic process.

Enhanced expression of ZNF521 *in human leukemic cell lines with t(17;19)*

To analyze the clinical significance of the three transcription factors identified in *EHKI*$^{\Delta Neo}$/MMLV leukemias (*Gfi1*, *Ikaros* and *Zfp521*) in human leukemia with t(17;19), we examined mRNA expression levels of the three genes in t(17;19)-positive (t(17;19)$^+$) ALL lines and in control B-lineage ALL lines without t(17;19). Cell lines were used instead of primary patient samples, because t(17;19)$^+$ ALL constitutes only a small subset of B-precursor leukemias (Look, 1997).

The results obtained using quantitative RT–PCR are shown in Figure 4. *Gfi1* mRNA levels were mostly constant in control and t(17;19)$^+$ cell lines, but the overall *Gfi1* expression in t(17;19)$^+$ lines was lower than that in control lines (Figure 4, left panel). As for *Ikaros*, mRNA expression levels were relatively stable in control lines but were varied among t(17;19)$^+$ lines, and the mean *Ikaros* expression in t(17;19)$^+$ lines was slightly lower than that in control lines (Figure 4, middle panel). These results indicated that the expression levels of *Gfi1* and *Ikaros* were not enhanced in t(17;19)$^+$ cell lines.

In contrast, the expression levels of *ZNF521*, the human homolog of *Zfp521* (also known as *early hematopoietic zinc-finger protein* (*EHZF*)), were found to be consistently higher in t(17;19)$^+$ lines than in control lines. Two lines showed approximately 10-fold upregulation and one line showed more than >50-fold upregulation (indicated by arrows and an arrowhead in the right panel of Figure 4). These results strongly suggest that the overexpression of *ZNF521* would be clinically relevant to t(17;19)-positive B-lineage ALL.

Expression of E2A-HLF *and* Zfp521 *conferred a growth advantage on B-progenitor cells, and both knocked-in for* E2A-HLF *and transgenic for* Zfp521 *mice developed B-lineage ALL*

We finally analyzed the *in vivo* cooperative role of *Zfp521* with *E2A-HLF*. For this purpose, we generated transgenic mice for *Zfp521* and crossed them with *EHKI*$^{\Delta Neo}$ mice. To express *Zfp521* in lymphoid cells, *Zfp521* complementary DNA with an *HA* tag (*Zfp521HA*) was subcloned into *EμSV* vector, which has been successfully used to express target genes in the lymphoid lineage (Rosenbaum *et al*., 1990) (Figure 5a). Among several transgenic lines established (*EμSV/Zfp521*), mice of a line that expresses *Zfp521HA* at a high level in lymphoid cells (data not shown) were chosen and crossed with *EHKI*$^{\Delta Neo}$ mice.

Figure 3 Retroviral integration sites, gene rearrangements and altered expression patterns in CISs detected in *EHKI*$^{\Delta Neo}$/MMLV leukemic mice (**a**) *Gfi1* gene. Upper panel: schematic illustrations of viral integration sites in the *Gfi1* gene. Exons are boxed, and the coding and non-coding regions are indicated by black and white boxes, respectively. Viral integration sites are indicated by vertical arrows with the related mouse identification numbers (nos. 1, 11, 6 and 8). Positions of probes used for Southern blot analyses are also shown. Lower left panel: Southern blot analysis for gene rearrangements. DNAs extracted from a control spleen (C) and *Gfi1*-integrated *EHKI*$^{\Delta Neo}$/MMLV mice (nos. 1, 11, 6 and 8) were digested with *Bam*HI and probed with the adjacent genomic fragment shown in (**a**) (probe A for nos. 1, 11 and 6, and probe B for no. 8). Germline (GL) and rearranged bands are indicated by arrows and arrowheads, respectively. Lower right panel: Northern blot analysis for *Gfi1* mRNA expression. mRNAs of a control spleen (C) and *Gfi1*-integrated *EHKI*$^{\Delta Neo}$/MMLV mice (nos. 1, 11, 6 and 8) were probed with the *Gfi1* coding region. *Gfi1*-non-integrated tumors (nos. 7 and 10) were also used as controls. The position of *Gfi1* mRNA is indicated by an arrow and *β-actin* hybridization served as the internal control. (**b**) *Ikaros* gene. Upper panel: schematic illustrations of virus integration sites in the *Ikaros* gene. Exons are boxed, and the coding and noncoding regions are indicated by black and white boxes, respectively. Viral integration sites are indicated by vertical arrows with the related mouse identification numbers (no. 3, 5 and 9). Positions of probes used for Southern blot analyses are also shown. Lower left panel: Southern blot analysis for gene rearrangements. DNAs extracted from a control spleen (C) and *Ikaros*-integrated *EHKI*$^{\Delta Neo}$/MMLV mice (nos. 3, 5 and 9) were digested with *Bam*HI and probed with the adjacent genomic fragment shown in (**a**) (probe C for nos. 3 and 5, probe D for no. 9). Germline (GL) and rearranged bands are indicated by arrows and arrowheads, respectively. Lower middle panel: Northern blot analysis for *Ikaros* mRNA expression. mRNAs of a control spleen (C) and *Ikaros*-integrated *EHKI*$^{\Delta Neo}$/MMLV mice (nos. 3, 5 and 9) were probed with the *Ikaros* coding region. *Ikaros*-non-integrated tumors (nos. 7 and 10) were also used as controls. The position of *Ikaros* mRNA is indicated by an arrow and *β-actin* hybridization served as the internal control. Lower right panel: RT–PCR for *Ikaros* mRNA isoforms. mRNAs of a control spleen (C) and *Ikaros*-integrated *EHKI*$^{\Delta Neo}$/MMLV mice (nos. 3, 5 and 9) were subjected to RT–PCR to detect *Ikaros* mRNA isoforms. The positions of isoforms *Ik1, Ik2, Ik3, Ik4 and Ik6* are indicated. A human CML BC cell line, BV173, was used to show the position of *Ik-6* (Nakayama *et al*., 1999). (**c**) *Zfp521* gene. Upper panel: Schematic illustrations of viral integration sites in the *Zfp521* gene. Exons are boxed, and the coding and noncoding regions are indicated by black and white boxes, respectively. Virus integration sites are indicated by vertical arrows with the related mouse identification numbers (nos. 2 and 4). Position of a probe used for Southern blot analyses is also shown. Lower left panel: Southern blot analysis of gene rearrangements. DNAs extracted from a control spleen (C) and *Zfp521*-integrated *EHKI*$^{\Delta Neo}$/MMLV mice (nos. 2 and 4) were digested with *Bam*HI and probed with the adjacent genomic fragment shown in (**a**) (probe E). Germline (GL) and rearranged bands are indicated by an arrow and arrowheads, respectively. Lower right panel: Northern blot analysis for *Zfp521* mRNA expression. mRNAs of a control spleen (C) and *Zfp521*-integrated *EHKI*$^{\Delta Neo}$/MMLV mice (nos. 2 and 4) were probed with the *Zfp521*coding region. *Zfp521*-non-integrated tumors (nos. 7 and 10) were also used as controls. Two alternatively spliced forms of *Zfp521* mRNA are indicated by arrows and *β-actin* hybridization served as the internal control.

Table 1 Characteristics of *EHKI*$^{Neo+}$/MMLV and *EHKI*$^{\Delta Neo}$/MMLV leukemic samples

Mouse no.	Age at disease (month)	PB parameters			Macroscopic tumor sites	Surface markers				Gene status		Diagnosis	Major integration site
		WBC ($\times 10^4/\mu l$)	Hb ($g\,dl^{-1}$)	Plt ($\times 10^4/\mu l$)		Thy1.2	B220	Gr1	Mac1	JH	TCRJ-β		
EHKI^{Neo+}/MMLV													
1	4.0	86.5	5.6	50.3	Thy, Spl	(+)	(−)	(−)	(−)	G/G	G/R	T-cell ALL	ND
2	4.5	25.1	16.7	26.3	Spl, LN	(−)	(−)	(−)	(−)	G/G	G/G	Lin$^-$ AL	ND
3	5.0	33.2	13.1	14.8	Thy, Spl	(+)	(−)	(−)	(−)	G/G	G/R	T-cell ALL	*Ahi1* (23rd intron)
4	5.3	15.1	13.5	28.5	Thy, Spl	(+)	(−)	(−)	(−)	G/G	G/R	T-cell ALL	*Ahi1* (9th intron)
5	5.5	67.5	7.1	44.9	Thy, Spl, LN	(+)	(−)	(−)	(−)	G/G	G/R	T-cell ALL	ND
6	6.0	15.3	12.5	38.8	Spl, LN	(−)	(−)	(−)	(−)	G/G	G/G	Lin$^-$ AL	ND
EHKI$^{\Delta Neo}$/MMLV													
1	2.6	16.3	10.0	30.3	Spl, LN	(−)	(−)	(−)	(−)	G/G	G/G	Lin$^-$ AL	*Gfi1* (5′ upstream)
2	3.1	16.0	14.0	46.1	Spl, LN	(−)	(+)	(−)	(−)	R/R	G/G	B-cell ALL	*Zfp521* (5′ noncoding)
3	3.2	1.0	4.7	7.1	Spl	(−)	(−)	(−)	(−)	G/G	G/G	Lin$^-$ AL	*Ikaros* (1st intron)
4	3.3	15.1	13.2	20.5	Spl, LN	(−)	(+)	(−)	(−)	R/R	G/G	B-cell ALL	*Zfp521* (5′ upstream)
5	3.3	21.3	12.2	41.2	Spl	(−)	(−)	(−)	(−)	G/G	G/G	Lin$^-$ AL	*Ikaros* (1st intron)
6	3.4	15.7	13.3	19.4	Spl	(−)	(−)	(−)	(−)	G/G	G/G	Lin$^-$ AL	*Gfi1* (3′ noncoding)
7	3.6	36.0	12.5	21.8	Spl, LN	(−)	(−)	(−)	(−)	G/G	G/G	Lin$^-$ AL	ND
8	3.8	54.9	11.5	16.7	Spl	(−)	(−)	(−)	(−)	G/G	G/G	Lin$^-$ AL	*Gfi1* (5′ upstream)
9	4.0	96.8	6.0	18.9	Spl, LN	(−)	(−)	(−)	(−)	G/G	G/G	Lin$^-$ AL	*Ikaros* (3rd intron)
10	4.5	20.5	5.3	20.2	Spl	(−)	(−)	(−)	(−)	G/G	G/G	Lin$^-$ AL	ND
11	5.6	2.1	2.7	51.9	Spl, LN	(−)	(−)	(−)	(−)	G/G	G/G	Lin$^-$ AL	*Gfi1* (5′ upstream)

Abbreviations: Ahi1, *Abelson helper integration site 1*; ALL, acute lymphoblastic leukemia; G, germline; *Gfi1*, *growth factor independent 1*; Hb, hemoglobin; *Ikaros*, *zinc-finger protein subfamily 1A1 isoform a* (*Zfp1a1*, also known as *Ikaros*); Lin$^-$, lineage marker-negative; LN, lympho node; Mac1, macrophage antigen-1; MMLV, Moloney murine leukemia virus; ND, not determined; PB, peripheral blood; plt, platelet; R, rearranged; Spl, spleen; Thy, thymus; WBC, white blood cell; *Zfp521*, *zinc-finger protein 521*.

The survival curves of the offspring are shown in Figure 5b. During about 6 months of observation period, half of the compound mice developed acute leukemia (thick continuous line), whereas none of *EHKI*$^{\Delta Neo}$ or *EμSV/Zfp521* alone showed hematological disease (thin continuous and thin dotted lines). All the leukemic cells were positive for B220 but negative for Thy1.2, Mac1 or Gr1 (data not shown) and showed rearrangement patterns in the *IgH* region (Figure 5c). The expression of *E2A-HLF* and *Zfp521HA* in the tumor tissues was confirmed by RT–PCR using primer sets specific for transcripts from *E2A-HLF* knocked-in allele (*E2A-77+HLF-2*, see Figure 1c) and *EμSV/Zfp521* transgene (*SV40-1+SV40-2*, see Figure 5a), respectively (Figure 5d).

As *EHKI*$^{\Delta Neo}$ mice with *Zfp521* overexpression exclusively developed B-lineage leukemia (nos. 1–5 of *EHKI*$^{\Delta Neo}$ × *EμSV/Zfp521HA* mice and nos. 2 and 4 of *EHKI*$^{\Delta Neo}$/MMLV mice), we analyzed the proliferative potential of B-progenitor cells in *EHKI*$^{\Delta Neo}$ mice and *EμSV/Zfp521* mice. For this purpose, BM cells extracted from both types of mice and their controls were subjected to flow cytometric analysis and B-cell colony formation assay. As shown in Figure 5e, both of *EHKI*$^{\Delta Neo}$ knock-in and *EμSV/Zfp521* transgenic BM cells contained increased number of B-cell precursors and possessed an enhanced B-cell colony formation ability when compared with those of control *EHKI*$^{Neo+}$ and *wild-type* mice (as for the results of flow cytometry, see also Supplementary Figure 3). These results indicated that expression of *E2A-HLF* and *Zfp521* rendered a proliferative ability to B-progenitor cells and suggest that their coexpression synergizes and contributes to the development of B-lineage leukemia.

Discussion

In earlier studies, we analyzed the role of *E2A-HLF* by a transgenic approach and showed that the expression of *E2A-HLF* under the control of lymphocyte-specific promoters perturbs normal lymphocyte development and contributes to the development of ALL (Honda *et al.*, 1999). However, in contrast with the fact that human leukemia harboring t(17;19) exclusively shows a B-cell phenotype, all the *E2A-HLF* transgenic mice developed T-cell ALL (Honda *et al.*, 1999). In this work, to circumvent this problem and to create a mouse model that further mimics human t(17;19)-positive ALL, we generated mice in which *E2A-HLF* was inducibly expressed under the control of the native *E2A* promoter.

Stimulation of *EHKI*$^{Neo+}$/*MxCre* mice with pIpC produced *EHKI*$^{\Delta Neo}$ mice, in which the deletion of the *floxed Neo* gene induced the expression of the *E2A-HLF* chimeric gene product in the hematopoietic tissues (Figures 1c and d). However, no disease was developed in *EHKI*$^{\Delta Neo}$ mice during the long-term observation period (Figure 2a, thin lines), indicating that the acquired expression of *E2A-HLF per se* is insufficient for the development of leukemia. This finding is in line with previous reports showing that iKI mice of other leukemogenic transcription factor chimeras, such as *AML1-ETO* and *MLL-CBP*, did not show hematopoietic disorders, and secondary mutations induced by *N*-methyl-*N*-nitrosourea or irradiation were required to induce a fully malignant phenotype (Higuchi *et al.*, 2002; Wang *et al.*, 2005). In this study, to introduce additional gene alterations, we used RIM, as it not only

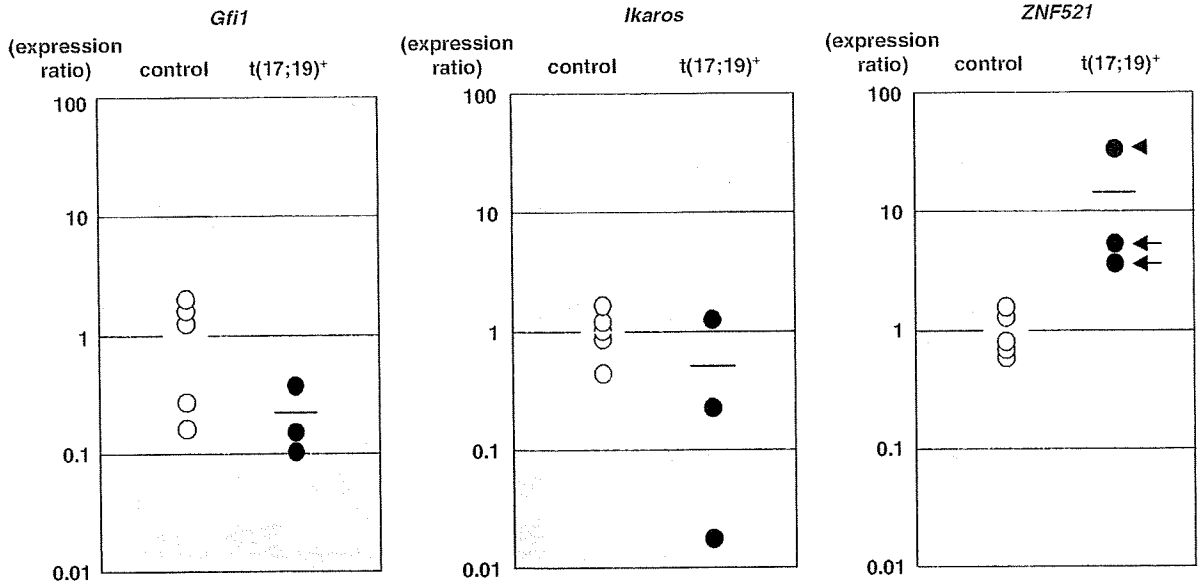

Figure 4 Quantitative mRNA expression of *Gfi1*, *Ikaros* and *ZNF521* in human leukemic cell lines with or without t(17;19). The mRNA expression levels in five control B-progenitor cell lines (control) and three t(17;19)-positive cell lines (t(17;19)$^+$) relative to the mean of the control cell lines (white bar) are indicated by white and black circles, respectively. The mean of t(17;19)$^+$ cell lines is indicated by a black bar. The relative expression ratio (vertical bar) is shown on a logarithmic scale. The high expression patterns of *ZNF521* in t(17;19)$^+$ cell lines are indicated by arrows and an arrowhead (right panel).

successfully induces mutations in the mouse genome but also has the advantage that the mutated genes can be detected by iPCR using the tumor genome and virus-specific primers (Jonkers and Berns, 1996; Mikkers and Berns, 2003; Nakamura, 2005).

MMLV infection induced acute leukemias in *EHKI*$^{\Delta Neo}$ mice at a higher frequency and with a shorter latency than in control *EHKI*$^{Neo\pm}$ mice (Figure 2a, thick lines). This finding indicates that *E2A-HLF* possesses an oncogenic potential in hematopoietic cells, which was accelerated by viral integrations. In addition, it is to be noted that the phenotypes of the leukemias were different between *EHKI*$^{\Delta Neo}$/MMLV and *EHKI*$^{Neo+}$/MMLV mice. In contrast with the fact that *EHKI*$^{Neo+}$/MMLV mice mainly developed T-cell ALL (four of six samples), *EHKI*$^{\Delta Neo}$/MMLV mice showed B-progenitor ALL (two samples) and lineage marker-negative leukemias (other nine samples; Figures 2b and c and Table 1).

Previous studies showed that that MMLV induces T-cell leukemia in wild-type mice very efficiently, at almost 100% penetrance (Jonkers and Berns, 1996; Mikkers and Berns, 2003). Thus, the reason why all the *EHKI*$^{Neo+}$/MMLV mice did not develop T-cell ALL is unclear. One possibility is the low copy number of the virus. This idea is supported by our previous RIM study, in which only ~60% of the MMLV-infected wild-type mice developed T-cell ALL (Mizuno *et al.*, 2008). In addition, it also remains to be clarified why leukemias of *EHKI*$^{\Delta Neo}$/MMLV mice showed B-progenitor and lineage marker-negative phenotypes. A previous report showed that transgenic background affected the disease phenotype of MMLV-induced leukemia. MMLV-infected wild-type mice exclusively developed T-ALL, whereas virus-infected *Eμ/bcl2* transgenic mice mainly succumbed to B-lineage leukemia (Shinto *et al.*, 1995). Therefore, it could be postulated that induced expression of *E2A-HLF* might exert its oncogenic potential in hematopoietic cells differentiating from a very early to the B-cell committed stage. This idea is in line with the finding that B-cell precursors in the *EHKI*$^{\Delta Neo}$ BM possessed a proliferative ability (Figure 5e) and is also in good agreement with the result that t(17;19)-positive human leukemia is exclusively of early B-progenitor phenotype (Inaba *et al.*, 1992).

Intriguingly, pathological analysis revealed that microthrombi, a clinical feature of coagulopathy, were observed in the lung of three *EHKI*$^{\Delta Neo}$/MMLV leukemic mice with relatively low platelet count (nos. 3, 6 and 8, indicated by arrows in Supplementary Figure 4, and see also Table 1). Microthrombus formation was not observed in control *EHKI*$^{Neo+}$/MMLV leukemic tissues and has not been detected in our previous RIM studies (Mizuno *et al.*, 2008; Miyazaki *et al.*, 2009), strongly suggesting that this pathological abnormality is specific for *E2A-HLF*-expressing leukemic mice. Taken together, our mouse model would not only reflect the oncogenicity of *E2A-HLF* in hematopoietic progenitor cells differentiating to the B-cell lineage (Inaba *et al.*, 1992), but also represent the coagulopathic property of t(17;19)-positive leukemic cells (Hunger, 1996).

iPCR of *EHKI*$^{\Delta Neo}$/MMLV leukemic mice identified *Gfi1*, *Ikaros* and *Zfp521* as CISs, whereas that of *EHKI*$^{Neo+}$/MMLV leukemic mice detected *Ahi1* as a CIS (Supplementary Tables 1 and 2). Major contribution of the CISs to tumor formation was confirmed

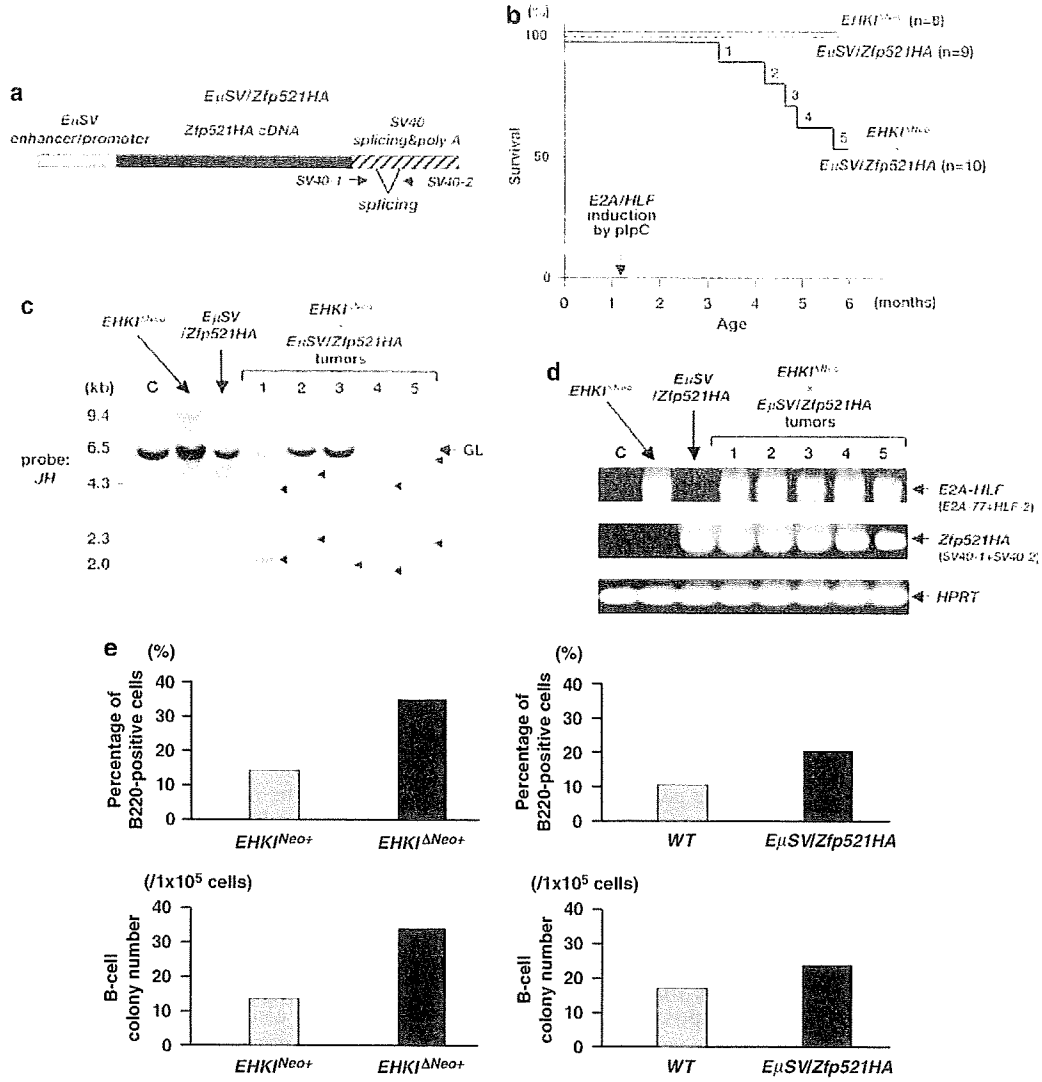

Figure 5 Cooperative oncogenecity of *Zfp521* with *E2A-HLF* and increased proliferative ability of B-cell precursors in *EHKI*$^{\Delta Neo}$ knock-in and *EμSV/Zfp521HA* transgenic mice. (**a**) Schematic structure of the transgene for generating *EμSV/Zfp521HA* transgenic mice. *EμSV enhancer/promoter*, *Zfp521HA* complementary (*c*)*DNA*, *SV40 splicing and polyA* signals are shown as gray, black and shaded boxes, respectively. The positions of the splicing and primers encompassing the splicing signal (*SV40-1* and *SV40-2*) are indicated. (**b**) Survival curves of *EHKI*$^{\Delta Neo}$ mice, *EμSV/Zfp521HA* mice and *EHKI*$^{\Delta Neo}$ × *EμSV/Zfp521HA* mice. During the observation period of 6 months, whereas no disease was observed in *EHKI*$^{\Delta Neo}$ and *EμSV/Zfp521HA* mice (thin continuous and thin dotted lines), half of *EHKI*$^{\Delta Neo}$ × *EμSV/Zfp521HA* mice died of leukemia (thick continuous line). The time point of *E2A-HLF* induction by pIpC is indicated by an arrow and the diseased *EHKI*$^{\Delta Neo}$ × *EμSV/Zfp521HA* mice are numbered. (**c**) Gene rearrangement analysis of leukemias developed in *EHKI*$^{\Delta Neo}$ × *EμSV/Zfp521HA* mice. DNAs extracted from a control spleen (C), an *EHKI*$^{\Delta Neo}$ mouse spleen, an *EμSV/Zfp521HA* mouse spleen and five tumors developed in *EHKI*$^{\Delta Neo}$ × *EμSV/Zfp521HA* mice were digested with *Eco*RI and blotted with the *JH* probe. Germline (GL) and rearranged bands are indicated by an arrow and arrowheads, respectively. (**d**) Expression of *E2A-HLF* and *Zfp521HA* in leukemias developed in *EHKI*$^{\Delta Neo}$ × *EμSV/Zfp521HA* mice. RNAs extracted from a control spleen (C), an *EHKI*$^{\Delta Neo}$ mouse spleen, an *EμSV/Zfp521HA* mouse spleen and five tumors developed in *EHKI*$^{\Delta Neo}$ × *EμSV/Zfp521HA* mice were subjected to RT–PCR for *E2A-HLF* (upper panel) and *Zfp521HA* (middle panel). All the tumors expressed both iKI allele- and transgenic allele-derived products. *HPRT* RT–PCR served as the internal control (lower panel). (**e**) Results of flow cytometric analysis (upper panels) and B-cell colony formation assay (lower panels). Upper panels: BM cells extracted from *EHKI*$^{Neo+}$ and *EHKI*$^{\Delta Neo}$ mice (left panels) and *wild-type* (*WT*) and *EμSV/Zfp521HA* mice (right panels) were analyzed by flow cytometry using anti-B220 and anti-Thy1.2 antibodies. The mean percentages of B220-positive cells of three independent mice are shown. Lower panels: BM cells extracted from the same types of mice were subjected to B-cell colony formation assay. The mean colony numbers of three independent mice are shown.

using Southern blot analysis (Figure 3 and Supplementary Figure 2), and aberrant expression of the gene products in the related leukemic tissues in *EHKI*$^{\Delta Neo}$/MMLV mice was shown using northern blot analysis (Figure 3). These results indicated that the three transcription factors, *Gfi1*, *Ikaros* and *Zfp521*, would have a cooperative role preferentially in *E2A-HLF*-mediated leukemogenesis.

Gfi1 was originally cloned as a gene whose activation in T-cells by MMLV insertion leads to IL-2 independence (Gilks *et al.*, 1993) and was subsequently found as a target in tumors that developed in MMLV-infected transgenic mice (Zörnig *et al.*, 1996; Scheijen *et al.*, 1997). Transgenic studies showed that the aberrant *Gfi1* expression itself does not efficiently induce leukemia, but exerts its oncogenic potential when coexpressed with other genes such as *Myc* or *Pim*. Thus, our results suggested that *E2A-HLF* might be a new candidate gene that cooperates with *Gfi1*.

The frequent retroviral integration in the *Ikaros* gene (3 of 11 samples, see Figure 3b and Table 1) is to be noted, as in a world-wide RIM screen (http://RTCGD.ncifcrf.gov), only four *Ikaros*-integrated samples were reported among more than several hundred CISs. A previous study using MMLV-infected *lck/NotchIC* (the active form of *Notch1*) transgenic mice identified *Ikaros* as a CIS (Beverly and Capobianco, 2003), in which MMLV was preferentially integrated in intron 2 and induced the expression of the dominant interfering *Ik-6*. However, in this study, the integration of MMLV in introns 1 or 3 increased expression of normal *Ikaros* isoforms (*Ik-1* to *Ik-4*) but did not induce *Ik-6* expression (Figure 3b). These results suggested that *Ikaros* might contribute to leukemogenesis through different mechanisms, depending on the partner genes.

Identification of *Zfp521* as a CIS is particularly interesting, as both *Zfp521*-integrated mice (nos. 2 and 4) developed B-progenitor ALL (Figure 2 and Table 1), which corresponds to the phenotype of human t(17;19)-positive leukemia. Therefore, it could be strongly postulated that *ZNF521*, the human counterpart of *Zfp521*, has an important role in the leukemogenic process of ALL with t(17;19). Indeed, among three zinc-finger proteins isolated as CISs in *EHKI*$^{\Delta Neo}$/MMLV leukemic mice, we found that only *ZNF521* was consistently overexpressed in human ALL cell lines harboring t(17;19) (Figure 4). In addition, both knocked-in for *E2A-HLF* and transgenic for *Zfp521* mice frequently developed B-lineage ALL (Figure 5), which showed the *in vivo* cooperative oncogenecity of *Zfp521* with *E2A-HLF*.

Zfp521 was originally identified as a retroviral integration site in AKXD mice with B-lineage lymphomas, which encodes a transcription factor with multiple zinc-fingers (Warming *et al.*, 2003). Although the molecular mechanisms by which aberrant expression of *Zfp521* contributes to leukemogenesis are not fully understood, one possibility is that Zfp521 impairs normal B-cell development by inhibiting the function of EBF1 (Hentges *et al.*, 2005), a transcription factor required for B-cell development (Lin and Grosschedl, 1995). Another possibility is that Zfp521 itself functions as a *trans*-repressor and perturbs normal hematopoietic cell development through a N-terminal conserved domain that recruits and interacts with the nucleosome remodeling and deacetylase corepressor complex (Bond *et al.*, 2008).

Zfp521 was found to be widely associated with B-cell leukemia/lymphoma in mouse, whereas aberrant expression of *ZNF521* is rarely found in B-progenitor ALL in human (Bond *et al.*, 2008). Considering that t(17;19)-positive leukemia is found in a small portion of human ALL (Look, 1997), it might be postulated that *Zfp521/ZNF521* is a preferential partner of *E2A-HLF* and the cooperative oncogenicity of these two genes constitutes a small subset of human B-lineage ALL.

In this report, we applied retrovirus insertional mutagenesis to *E2A-HLF* iKI mice, isolated *Gfi1*, *Ikaros* and *Zfp521* as cooperative genes with *E2A-HLF* and identified *Zfp521/ZNF521* to be a cooperative gene for *E2A-HLF* in t(17;19)-positive B-lineage leukemia. These results provide evidence that multi-step gene alterations are required for leukemogenesis and prove that the iKI system in conjugation with RIM is a valuable tool for identifying genes whose aberrant expression contributes to the malignant transformation of hematopoietic cells.

Materials and methods

Construction of iKI and transgenic vectors and generation of knock-in and transgenic mice
Detailed procedures for construction of iKI and transgenic vectors and for generation of iKI and transgenic mice are described in Supplementary Table 3.

Primer sequences
All the primer sequences used in this study are shown in Supplementary Table 4.

RT–PCR
To detect *E2A-HLF* mRNA, RT–PCR was performed using *E2A-77* and *HLF-2* primers that were derived from *E2A* exon 1 and the *HLF* portion of *E2A-HLF* complementary DNA as previously described (Miyazaki *et al.*, 2002). *Zfp521* mRNA expression was examined by RT–PCR using *SV40-1* and *SV40-2* primers that encompass the *SV40 splicing* signal as described (Honda *et al.*, 1995). To detect *Ikaros* mRNA isoforms, RT–PCR was performed as described elsewhere (Nakayama *et al.*, 1999). To quantitate mRNA expression in human cell lines and mouse tissues, quantitative RT–PCR was performed using primers listed in Supplementary Table 4 as previously described (Miyazaki *et al.*, 2002).

Immunoprecipitation and western blot
Tissues were homogenized in 1% Triton lysis buffer and immunoprecipitation and western blot were performed as previously described (Honda *et al.*, 1999). Positive signals were visualized using enhanced chemiluminescence.

MMLV infection and identification of retroviral integration sites
Preparation and infection of retroviruses were performed as previously described (Wolff *et al.*, 2003a, b). Identification of retroviral integration sites was performed essentially as described elsewhere (Yamashita *et al.*, 2005). Position mapping on the mouse chromosome was performed with a Basic Local Alignment Search Tool (BLAST) search using the University of California Santa Cruz Genome Bioinformatics database (http://genome.ucsc.edu) and the definition of a CIS was the same as in the retrovirus tagged cancer gene database (http://RTCGD.ncifcrf.gov) (Akagi *et al.*, 2004).

Pathological and flow cytometric analyses
Smears and stamp specimens of leukemic tissues were examined as described (Honda *et al.*, 1999). Flow cytometric analysis were performed as previously described (Miyazaki *et al.*, 2009).

Colony assays

Colony assays were performed as previously described (Miyazaki *et al.*, 2009). In brief, 1×10^5 BM cells were subjected for a B-cell colony formation assay using MethoCult M3630 (StemCell Technologies, Inc., Vancouver, Canada), which contains 10 ng/ml rhIL-7. After 12–14 days of incubation, colony numbers were counted.

Conflict of interest

The authors declare no conflict of interest.

Acknowledgements

We thank Yuki Sakai, Kayoko Hashimoto, Yuko Tsukawaki and Rika Tai, for the care of the mice and technical assistance, Dr Nobuaki Yoshida for E14 ES cells, Dr Søren Warming, Dr Neal G Copeland and Dr Nancy A Jenkins for mouse *Zfp521* cDNA, Dr Koichi Ikuta for mouse *TCRJβ* probe, Dr Hirotaka Matsui for statistical analysis and Dr Takuro Nakamura for helpful discussion. This work was in part supported by a grant-in-aid from the Ministry of Education, Science and Culture of Japan, a grant-in-aid for Cancer Research from the Ministry of Health, Labour and Welfare of Japan (13-2), Takeda Science Foundation, Astellas Foundation for Research on Metabolic Disorders, the Japan Leukaemia Research Fund and Tsuchiya Foundation.

Authorship

Contribution: NY, Z-iH, TI and HH designed and performed the research and wrote the paper; HO centralized the pathological analysis; RK and LW generated the retrovirus; KM, MM and TS participated in the flow cytometric analysis; AN performed colony assays. All the authors checked the final version of the paper.

References

Akagi K, Suzuki T, Stephens RM, Jenkins NA, Copeland NG. (2004). RTCGD: retroviral tagged cancer gene database. *Nucleic Acids Res* **32**: (Database issue) D523–527.

Aspland SE, Bendall HH, Murre C. (2001). The role of E2A-PBX1 in leukemogenesis. *Oncogene* **20**: 5708–5717.

Bain G, Engel I, Robanus Maandag EC, te Riele HP, Voland JR, Sharp LL *et al.* (1997). E2A deficiency leads to abnormalities in alphabeta T-cell development and to rapid development of T-cell lymphomas. *Mol Cell Biol* **17**: 4782–4791.

Bain G, Maandag EC, Izon DJ, Amsen D, Kruisbeek AM, Weintraub BC *et al.* (1994). E2A proteins are required for proper B cell development and initiation of immunoglobulin gene rearrangements. *Cell* **79**: 885–892.

Beverly LJ, Capobianco AJ. (2003). Perturbation of Ikaros isoform selection by MLV integration is a cooperative event in Notch(IC)-induced T cell leukemogenesis. *Cancer Cell* **3**: 551–564.

Bond HM, Mesuraca M, Amodio N, Mega T, Agosti V, Fanello D *et al.* (2008). Early hematopoietic zinc finger protein-zinc finger protein 521: a candidate regulator of diverse immature cells. *Int J Biochem Cell Biol* **40**: 848–854.

Dang J, Inukai T, Kurosawa H, Goi K, Inaba T, Lenny NT *et al.* (2001). The E2A-HLF oncoprotein activates Groucho-related genes and suppresses Runx1. *Mol Cell Biol* **21**: 5935–5945.

Gilks CB, Bear SE, Grimes HL, Tsichlis PN. (1993). Progression of interleukin-2 (IL-2)-dependent rat T cell lymphoma lines to IL-2-independent growth following activation of a gene (Gfi-1) encoding a novel zinc finger protein. *Mol Cell Biol* **13**: 1759–1768.

Hentges KE, Weiser KC, Schountz T, Woodward LS, Morse HC, Justice MJ. (2005). Evi3, a zinc-finger protein related to EBFAZ, regulates EBF activity in B-cell leukemia. *Oncogene* **24**: 1220–1230.

Higuchi M, O'Brien D, Kumaravelu P, Lenny N, Yeoh EJ, Downing JR. (2002). Expression of a conditional AML1-ETO oncogene bypasses embryonic lethality and establishes a murine model of human t(8;21) acute myeloid leukemia. *Cancer Cell* **1**: 63–74.

Honda H, Fujii T, Takatoku M, Mano H, Witte ON, Yazaki Y *et al.* (1995). Expression of p210bcr/abl by metallothionein promoter induced T-cell leukemia in transgenic mice. *Blood* **85**: 2853–2861.

Honda H, Inaba T, Suzuki T, Oda H, Ebihara Y, Tsuiji K *et al.* (1999). Expression of E2A-HLF chimeric protein induced T-cell apoptosis, B-cell maturation arrest, and development of acute lymphoblastic leukemia. *Blood* **93**: 2780–2790.

Hunger SP. (1996). Chromosomal translocations involving the E2A gene in acute lymphoblastic leukemia: clinical features and molecular pathogenesis. *Blood* **87**: 1211–1224.

Inaba T, Inukai T, Yoshihara T, Seyschab H, Ashmun RA, Canman CE *et al.* (1996). Reversal of apoptosis by the leukaemia-associated E2A-HLF chimaeric transcription factor. *Nature* **382**: 541–544.

Inaba T, Roberts WM, Shapiro LH, Jolly KW, Raimondi SC, Smith SD *et al.* (1992). Fusion of the leucine zipper gene HLF to the E2A gene in human acute B-lineage leukemia. *Science* **257**: 531–534.

Inukai T, Inaba T, Yoshihara T, Look AT. (1997). Cell transformation mediated by homodimeric E2A-HLF transcription factors. *Mol Cell Biol* **17**: 1417–1424.

Inukai T, Inoue A, Kurosawa H, Goi K, Shinjyo T, Ozawa K *et al.* (1999). SLUG, a ces-1-related zinc finger transcription factor gene with antiapoptotic activity, is a downstream target of the E2A-HLF oncoprotein. *Mol Cell* **4**: 343–352.

Jonkers J, Berns A. (1996). Retroviral insertional mutagenesis as a strategy to identify cancer genes. *Biochem Biophys Acta* **1287**: 29–57.

Kuhn R, Schwenk F, Aguet M, Rajewsky K. (1995). Inducible gene targeting in mice. *Science* **269**: 1427–1429.

Kurosawa H, Goi K, Inukai T, Inaba T, Chang KS, Shinjyo T *et al.* (1999). Two candidate downstream target genes for E2A-HLF. *Blood* **93**: 321–332.

Lin H, Grosschedl R. (1995). Failure of B-cell differentiation in mice lacking the transcription factor EBF. *Nature* **376**: 263–267.

Look AT. (1997). Oncogenic transcription factors in the human acute leukemias. *Science* **278**: 1059–1064.

Matsunaga T, Inaba T, Matsui H, Okuya M, Miyajima A, Inukai T *et al.* (2003). Regulation of annexin II by cytokine-initiated signaling pathways and E2A-HLF oncoprotein. *Blood* **103**: 3185–3191.

Mikkers H, Berns A. (2003). Retroviral insertional mutagenesis: tagging cancer pathways. *Adv Cancer Res* **88**: 53–99.

Miyazaki K, Kawamoto T, Tanimoto K, Nishiyama M, Honda H, Kato Y. (2002). Identification of functional hypoxia response elements in the promoter region of the DEC1 and DEC2 genes. *J Biol Chem* **277**: 47014–47021.

Miyazaki K, Yamasaki N, Oda H, Kuwata T, Kanno Y, Miyazaki M *et al.* (2009). Enhanced expression of p210BCR/ABL and aberrant expression of Zfp423/ZNF423 induce blast crisis of chronic myelogenous leukemia. *Blood* **113**: 4702–4710.

Mizuno T, Yamasaki N, Miyazaki K, Tazaki T, Koller R, Oda H *et al.* (2008). Overexpression/enhanced kinase activity of BCR/ABL and altered expression of Notch1 induced acute leukemia in p210BCR/ABL transgenic mice. *Oncogene* **27**: 3465–3474.

Nakamura T. (2005). Retroviral insertional mutagenesis identifies oncogene cooperation. *Cancer Sci* **96**: 7–12.